SYNTHESIS AND CHARACTERIZATION OF ACTIVATED CARBON ZEOLITE COMPOSITE FROM COAL FLY ASH FOR Pb (II) REMOVAL FROM AQUEOUS SOLUTION

A DISSERTATION SUBMITTED FOR THE PARTIAL FULFILLMENT OF THE REQUIREMENTS FOR THE MASTER OF SCIENCE DEGREE IN CHEMISTRY

BY

Mahesh Regmi

Exam Roll No.: 137/2071

Registration No.: 5-2-37-100-2010

Submitted To

CENTRAL DEPARTMENT OF CHEMISTRY

INSTITUTE OF SCIENCE AND TECHNOLOGY,

TRIBHUVAN UNIVERSITY, KIRTIPUR, KATHMANDU, NEPAL

May 24, 2018

BOARD OF EXAMINER AND CERTIFICATE OF APPROVAL

This dissertation entitled "**Synthesis and Characterization of Activated Carbon Zeolite Composite from Coal Fly Ash for Pb (II) Removal from Aqueous Solution**" by "Mahesh Regmi", under the supervision of Professor Dr. Vinay Kumar Jha, University Campus, Central department of Chemistry, Tribhuvan University, Nepal, is hereby submitted for the partial fulfillment of the Master of Science (M.Sc.) degree in Chemistry. This dissertation has not been submitted in any other university or institution previously for the award of a degree.

_____

(Professor Dr. Vinay Kumar Jha)

Supervisor

Central Department of Chemistry

Tribhuvan University, Kirtipur, Kathmandu, Nepal

_____

(Professor Dr. Amar Prasad Yadav)

Internal Examiner

Central Department of Chemistry

Tribhuvan University, Kirtipur, Kathmandu, Nepal

_____

(Professor Dr. Rejina Maskey Byanju)

External Examiner

Central Department of Environmental Science

Tribhuvan University, Kirtipur, Kathmandu, Nepal

_____

(Professor Dr. Ram Chandra Basnyat)

Head of the Department

Central Department of Chemistry

Tribhuvan University, Kirtipur, Kathmandu, Nepal

Date: May 24, 2018

RECOMMENDATION LETTER

This is to certify that the dissertation work entitled **"Synthesis and Characterization of Activated Carbon Zeolite Composite from Coal Fly Ash for Pb (II) Removal from Aqueous Solution"** has been carried out by **"Mahesh Regmi"** as a partial fulfillment for the requirement of M.Sc. Degree in Chemistry under my supervision. To the best of my knowledge, this work has not been submitted to any other degree in this institution.

_____

(Professor Dr. Vinay Kumar Jha)

Supervisor

Central Department of Chemistry

Tribhuvan University, Kirtipur, Kathmandu, Nepal

Date: May 24, 2018

DECLARATION

I, **"Mahesh Regmi"**, hereby declare that the work presented here is genuine work done originally by me and has not been published or submitted elsewhere for the requirement of a degree program. Any literature, data or works done by others and cited in this dissertation has been given due acknowledgement and listed in the reference section.

_____

"Mahesh Regmi"

Date: May 24, 2018

ACKNOWLEDGEMENTS

It is a matter of immense pleasure that I got an opportunity to do this dissertation work under the supervision of Prof. Dr. Vinay Kumar Jha, Professor of Central Department of Chemistry, Tribhuvan University. I would like to express my sincere gratitude to him for his constant support, guidance, care and valuable suggestions.

I would like to express my sincere gratitude to Professor Dr. Megh Raj Pokhrel, former Head of the Department, Central Department of Chemistry for inspiration and providing me the golden opportunity and necessary physical facilities for this dissertation work. I am also thankful to present Head of the Department Prof. Dr. Ram Chandra Basnyat.

I am thankful to Department of Environment, Government of Nepal, Ministry of Forests and Environment for providing grant to carry out my research work.

Further, I am glad to thank all the teaching and non-teaching staff of Central Department of Chemistry. I would also like to thank my entire friend for their help during the research work.

Similarly, I am grateful to Mr. Manoj Rana, Department of Mines and Geology, Government of Nepal for providing necessary laboratory facilities to conduct the dissertation work.

Lastly, I would like to remember my parents Tanka Prasad Regmi and Kalpana Regmi, especially my sister Laxmi Regmi, Sabitri Regmi and wife Madhavi Mishra for their precious contribution and dedication in my research work.

Mahesh Regmi

May 24, 2018

ABBREVIATIONS

AAS	=	Atomic absorption spectroscopy
b	=	Langmuir constant in L/mg
C_e	=	Equilibrium concentration of Lead in mg/g
C_i	=	Initial concentration of metal in mg/L
CFA	=	Coal Fly ash
EPA	=	Environmental protection agency
FTIR	=	Fourier transform infra-red
K_1	=	Pseudo-first order rate constant in min^{-1}
K_2	=	Pseudo-second order rate constant in g mg^{-1}
Mt	=	Metric ton
ppb	=	Parts per billion
ppm	=	Parts per million
Q_e	=	Amount adsorbed at equilibrium time in mg/g
Q_m	=	Amount of metal to form monolayer coverage in mg/g
Q_t	=	Amount adsorbed at time t in mg/g
R^2	=	Correlation coefficient
WHO	=	World Health organization
XRD	=	X-ray diffraction

ABSTRACT

The present work deals with the preparation of activated carbon zeolite composite by activating Coal Fly ash (CFA) with NaOH at 650 ºC in N_2 atmosphere followed by heating at 80 ºC for 24 hrs. The heavy metal removal performance of the obtained fly ash based zeolite was investigated in Pb^{2+} removal experiments. Lead (Pb^{2+}) is a positively charged toxic pollutant that can be present in surface water and industrial waste water and may cause harmful physiological effects to human beings. Since zeolites have an inherent negative charge in their framework, they are capable of removing heavy metal from water. The activated carbon zeolite composite were characterized by XRD analysis, FTIR and methylene blue adsorption method. The XRD peaks at 2θ values of 33 and 35º were due to $NaAlO_2$ and 26-29 and 45º were due to $NaAlSiO_4$ which shows the strong evidence for the formation of zeolitic product. The AAS was employed for Pb analysis. For Lead (II) ion adsorption, the effect of pH, initial concentration and reaction time were studied. The optimum pH for Lead (II) ion adsorption was found to be 6. The value of ΔG was -24.00 kJ/mole which confirmed the adsorption process was spontaneous and favored by physio-chemical adsorption. The value of χ^2 for the Langmuir model was smaller than that of the Freundlich model and the correlation coefficient value for Langmuir plot was more approaching to 1 than that of Freundlich plot which concludes that adsorption of Lead (II) on activated carbon-zeolite follows the Langmuir adsorption isotherm. The equilibrium monolayer adsorption capacity calculated from Langmuir model was 270.270 mg/g. The adsorption reached equilibrium in 120 minutes and the kinetics data fit well to pseudo second order model with the rate constant value of 0.0056 g/(mg.min).

Keywords: Activated carbon-zeolite composite; Adsorption isotherms; Coal Fly ash; Lead (II) ion; Rate constant

TABLE OF CONTENTS

CHAPTER 1

INTRODUCTION

1.1 General Introduction

The backbone of modern civilization and industry is based on thermal power, heat and energy in various forms. The energy industry is by far the biggest in the world. In the energy industry, coal powered thermal plants is one of the major players. It is also one of the major polluters in the world. As in any chemical industries there are multiple polluting items and agents hence cannot be generalized. In light of that the key polluting waste generated in thermal plants is identified as coal fly ash (CFA)[1].

There are several impacts of CFA into terrestrial ecosystem. Leaching of toxic elements into soil and ground water. The toxic elements may enters plants through ground water and contaminate the whole food cycles of plants, animals, humans and fishes[2]. The dumping of CFA in ash damps and ponds has direct effects in aquatic life because of ground water pollution. The primary change associated with water chemistry includes pH variations and increase in concentrations level of toxins in water[3].

The management of CFA becomes both economic and environmental issues. Several technological options have been proposed for the disposal of fly ash such as the use of raw materials substitute in the cement production. As the major component of CFA is amorphous aluminosilicate, the conversion of CFA to zeolite has been proposed as a viable method. This is not only to generate a useful adsorbent but also to increase the value of industrial waste CFA[4].

Zeolites are crystalline inorganic polymer, or better said three dimensional porous aluminosilicate compounds, consisting of 3-dimensional arrangement of $[SiO_4]^{4-}$ and $[AlO_4]^{5-}$ polyhedral connected through their oxygen atoms to form a negatively charge lattice due to isomorphous substitution of Si^{4+} by Al^{3+}. In order to maintain electro neutrality mobile counter cations are stored in an intravoidal water of the zeolite solids[5-7]. The general formulas of zeolites are expressed below:

$$M_{x/n}\,[(AlO_2)_x \cdot (SiO_2)_y] \cdot w\,(H_2O)$$

Where M is a cation of valence n that balances the negative charges associated with the aluminum tetrahedral, the terms x and y correspond to the stoichiometric coefficients of the alumina and silica tetrahedral and w is the number of water molecules.

The fascinating properties of zeolitic material, such as their ion exchange properties, their sorption capacity, their shape selectivity, their catalytic activity, or their role as hosts in advance materials, are determined by their crystal structure. Sorption characteristics depend upon the size of the pore openings and the void volume and ion-selectivity upon the number and nature of the cation sites and their accessibility. Therefore, an important aspect of zeolite science is structural analysis[8].

Zeolites are categorized into natural and synthesized types. Usually, synthesized zeolites are preferred over natural ones due to the possibility of adjusting their pore size through different synthesizing techniques. Different zeolites are synthesized from CFA among which A, X and Y are more valuable because of their extensive catalytic application in detergent, petroling refining and petrochemical industries. The two most common methods available for this conversion are hydrothermal method and fusion method where the fusion method has advantages on the speed of the reaction and the purity of the final products whereas the hydrothermal provides a more consistent pattern of zeolite products[9].

Environmental friendly utilization of CFA is an important subject because of measures needed for the prevention of environmental pollution. Although zeolites synthesis from fly ash is a minor application, it has begun to attract more attention because zeolites are useful materials for environmental remediation. Surface water pollution which is rapidly increasing with industrialization and urbanization has become a global environmental problem. In particular, severe problems arise from contamination of water by heavy metal ions and ions such as ammonium and phosphate which cause Eutropication[10].

The hydrothermal treatment with NaOH solution is a promising technique for the conversion of CFA into zeolites. Further approaches involving hydrothermal treatment, such as the two step method (fusion followed by hydrothermal treatment) and the dry or molten salt method have been developed in order to achieve high synthesis efficiency and

high crystallinity. The application of microwave synthesis has also been shown to be effective in reducing the reaction time.

The different zeolites synthesized from fly ash are given in **Table 1.1**[11].

Table 1.1: Some common zeolites synthesized from Fly ash

zeolite	**Chemical formula**
Zeolite-A	$NaAlSi_{1.1}O_{4.2}\cdot 2.25H_2O$
Zeolite-P	$Na_6Al_6Si_{10}O_{32}\cdot 12H_2O$
Zeolite-X	$NaAlSi_{1.23}O_{4.46}\cdot 3.07H_2O$
Zeolite-Y	$NaAlSi_{2.43}O_{6.86}\cdot 4.46H_2O$
Phillipsite	$K_2Al_2Si_3O_{10}\cdot H_2O$
Mordenite	$Na_2Al_2Si_{3.3}O_{8.8}\cdot 6.7H_2O$
Hydroxysodalite	$Na_{1.08}Al_2Si_{1.68}O_{7.44}\cdot 1.8H_2O$
Analcime	$NaAlSi_2O_6\cdot H_2O$
K- Chabazite	$KAlSiO_4\cdot 1.5H_2O$
Hydroxycancrinite	$Na_{14}Al_{12}Si_{13}O_{51}\cdot 6H_2O$

Zeolites have an open structure that accommodates a variety of cations, such as Na^+, K^+, Ca^{2+} and Mg^{2+}, as well as mobile water molecules that can be readily loss and regained, accounting for their desiccant properties. The loosely bound positive ions can be readily exchanged for others in aquatic environment. This gives the porous structure ability of ion exchange. The ratio of silica to alumina commonly varies between one and five, giving different composition[12-14]. The idealized zeolite framework structure is presented in **Fig. 1.1**[15].

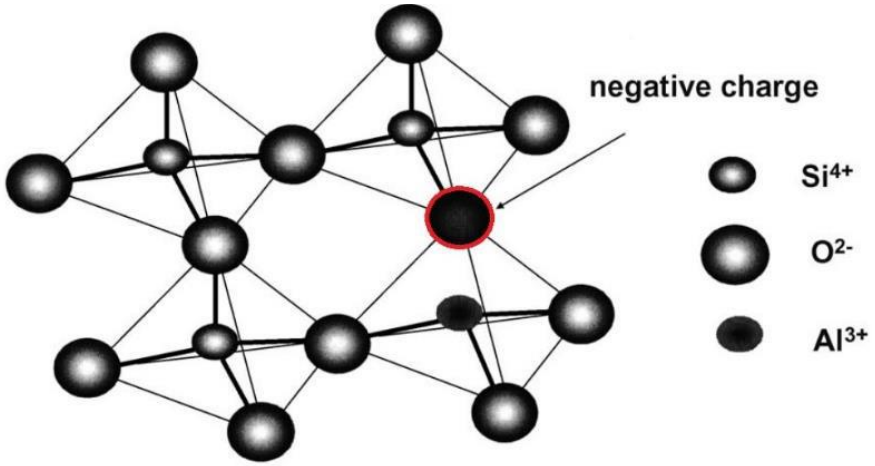

Fig. 1.1: Idealized structure of Zeolite-Si/Al substitution yielded a negative charge on framework

A framework type describes the connectivity of the tetrahedrally coordinated atoms of the framework in the highest possible symmetry. Therefore, many different materials can be classified under one designation. A three-letter code is assigned to confirm framework types by the International zeolite association. The codes are normally derived from the name of the zeolite, e.g. FAU from the minerals Faujasite, and LTA from Linde Type A. The description of the zeolite structure mostly begins with the description of framework type in terms of pore opening size and dimensionality of the channel system. Pore opening are characterized by the size of the ring that define the pore designated an n ring where n is equal to the number of T atoms (tetrahedrally coordinated cations) and O-atoms in the ring. An 8 ring is considered a small pore opening, a 10 ring being medium and a 12 ring a large one with effective pore width of 0.41, 0.55 and 0.74 nm respectively (calculated using oxygen radii of 0.135 nm).

Some structural features (cages, channels, chain and sheets) are common to several different zeolitic frameworks. Some of these subunits are shown in **Fig 1.2**. For example, sodalite cage is a truncated octahedron whose surface is defined by six 4 rings and eight 6 rings, therefore sodalite would be designated as $4^6 6^8$ cage[8,14,16].

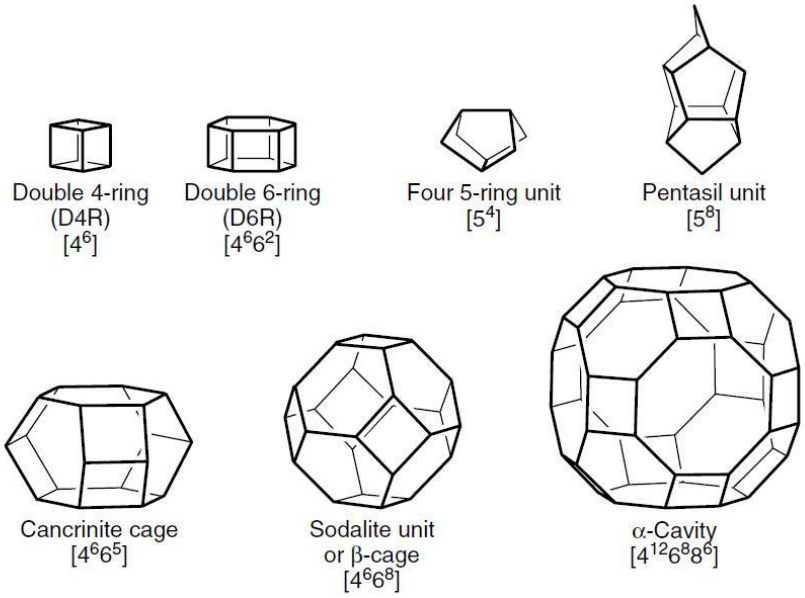

Fig. 1.2: Some subunits and cavities seen in many framework and types

The stacking sequence of layers, cages, or rings in zeolite frameworks is often described using "ABC" system. The terminology for crystal chemistry is normally used to describe the stacking of layers of closed packed spheres (atoms). This concept is not only a way to describe a family of framework, but also reflect the way nature builds real materials with such frameworks. Although, there are 232 confirmed zeolites framework types (as of 2016), only a few of them describe zeolites that are used in industrial application. The best description of SOD framework is "a body centered cubic arrangement of β-or sodalite-cages joined through shared 4-and 6-rings" and can be viewed as an ABC ABC stacking hexagonal arrays of single 6 rings in the [111] directions.

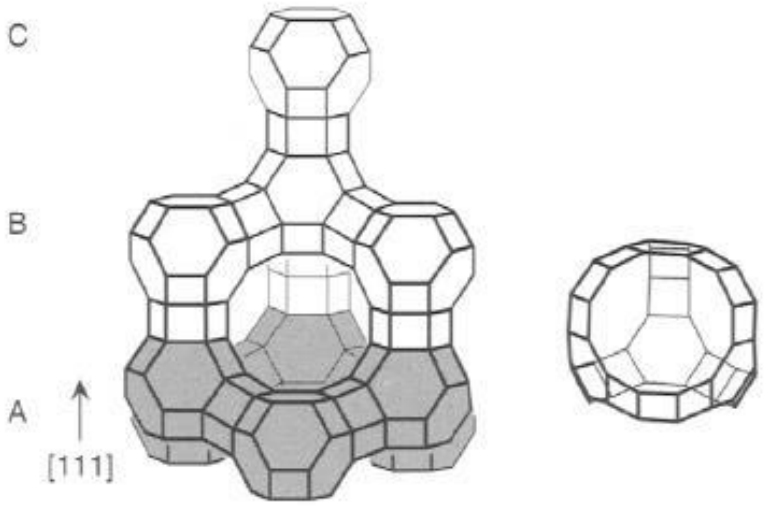

Fig. 1.3: Na-X Zeolite with FAU Framework type and Supercage

The LTA framework type consists of primitive cubic arrangement of sodalite cages via Oxygen bridge to form 4 double ring. This creates an α-cavity and a three dimensional 8 ring channel system. Zeolite A is a technologically important porous zeolite which is widely used for various separation and purification applications. Zeolite A in its synthesized form (molecular sieve 4A) has the unit cell formula $Na_{12}(AlO_2)_{12}.nH_2O$. Sodium ions can be exchanged by Calcium, Silver, Potassium, or other metal ions to yield adsorbents with desired properties[8].

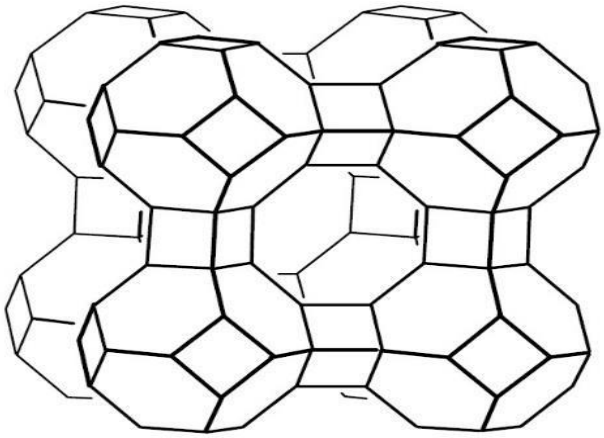

Fig. 1.4: The LTA Framework type

Waste water discharged by industries that process non-ferrous metal ores and concentrater are usually polluted with heavy metal ions such as Cd^{2+}, Pb^{2+}, Ni^{2+}, Cu^{2+}, Zn^{2+} etc. Many industries involved in metal finishing, mining and mineral processing, coal mining and oil refining, have problem associated with heavy metal contamination of process and run off waters. The development of new approaches and technologies is therefore needed for both the removal and recovery of valuable metals from waste waters[10].

Lead is ubiquitous in the environment and hazardous at high levels. Lead is a chemical element in the group IV A of periodic table with symbol Pb [At. No. 82., At. Wt. 207.2., Density. 11.34 g/cm^3., M. P. 327.46 ºC and B. P. 1749 ºC]. Lead is a soft, malleable and heavy post-transition metal. Metallic lead has a bluish-white color after being freshly cut, but it soon tarnishes to a dull grayish color when exposed to air. Leads are introduced in the atmosphere due to the use of pesticides containing Lead[17].

Lead is recognized as a longstanding environment pollutant. It can be found in waste water generated by various industries such as bullet and shot, fusible alloys, acid battery, ceramics and glass manufacturing, metal planting and finishing, printing, tanning and production of lead additives for gasoline[18]. Discarded electrical and electronic products are called e-waste and lead is the typical representative of e-waste which has generated both toxic and valuable materials for society[19]. Lead acid batteries are the important source of lead as water pollutant in Nepal due to its growing use especially after the government's encouragement to use solar power in an attempt to save electricity. Improper dumping of such used lead acid batteries can contaminate the surrounding environment with lead[20].

Lead has no biological use and it is highly toxic to all living beings even in relatively low concentrations. So, environmentalist and medical scientists have given special attention towards research Pb (II) ion contamination in water[21]. Drinking water of 10, 10 15 and 10 ppb of Lead is considered to be safe by the World Health Organization (WHO), the European Union (EU), the United States Environmental Protection Agency (USEPA) and Guidelines for Canadian Drinking water Quality, respectively[22]. Lead is a general metabolic or systemic poison and enzyme inhibitors which can accumulate in brain, bones, muscles and kidney. So, drinking water containing high level of lead for a long time can cause serious disorders, such as anemia, kidney disease, sterility, abortion neonatal death and mental retardations[23]. Therefore removal of Lead from waste water prior to discharge into environment is necessary.

Reverse osmosis and electrodialysis, chemical precipitation, ion exchange, membrane filtration and carbon adsorption are the main techniques for treating contaminated waste water streams containing heavy metals including Lead. Adsorption technology is cost effective and environmental friendly. So, it is considered as universal and an efficient method of water treatment as per the guidelines of WHO and EPA. The cost effectiveness of this technology is due to the use of effective adsorbents by converting solid waste to value-added products[24].

1.2 Adsorption Studies

The phenomenon of increasing the concentration of substance on the surface of a solid or liquid than in the bulk of solid or liquid is called adsorption. The substance onto which adsorption takes place is called adsorbent and the substance which gets adsorbed

(attached) onto the other surface is called adsorbate. Adsorption is a surface phenomenon and at a given temperature and pressure depends on the surface area of the adsorbent[25]. The term adsorption is used to describe the fact that there is a greater concentration of adsorbed molecules on the surface of solid than in the gas phase or bulk solution[26]. The adsorption can be studied in batch adsorption and column adsorption modes.

In column experiment, a column of a particular length and internal diameter is set up. A porous sheet is attached at the bottom of the column in order to support the adsorbent to ensure the uniform inlet flow and good liquid distribution into the column. The effluent is allowed to flow through the column at constant flow rate using flow controller. The adsorbate concentrations before and after adsorption are measured using appropriate method. The operation of the column is stopped when the effluent adsorbate concentration reaches a constant value.

In batch adsorption experiment, a definite mass of adsorbent is mixed with the predetermined volume and concentration of pH adjusted adsorbate solution into the corked conical flasks. The flasks are shaken vigorously in a mechanical shaker at room temperature for 24 hours to attain adsorption equilibrium. The initial and equilibrium concentrations of adsorbate are determined using appropriate method. The adsorption of species ion of interest onto the adsorbent is affected by different parameters such as initial concentration, contact time and pH of the solution[27]. By varying any one parameters and keeping the other parameters constant, the effect of each parameter can be studied.

From the adsorbate concentration determined before and after adsorption C_i and C_e respectively and dry weight of adsorbent W, the volume of sample (V), the amount of adsorbate adsorbed Q (mg/g) at equilibrium is computed by the following formula

$$C_e = \frac{(C_i - C_e)V}{W} \qquad \ldots\ldots\ldots \quad (1.1)$$

Adsorbate removal percentage is calculated from the ratio of decrease in Concentration before and after adsorption to the initial Concentration of solution. Therefore adsorption percentage is given by

$$\text{Removal } \% = \frac{C_i - C_e}{C_e} \times 100\% \quad \cdots\cdots \quad (1.2)$$

The distribution ratio D for the adsorption process at equilibrium is determined by following equation:

$$D = \frac{Q_e}{C_e} \quad \cdots\cdots \quad (1.3)$$

Where Q_e and C_e are the equilibrium amount and the equilibrium concentration of ion of interest respectively.

1.3 Methods for the Determination of Specific Surface Area

There are several methods for the determination of specific surface area of the activated carbons. Some may be tedious and expensive while others are easy and cheap. Following are some of the methods for specific surface area determination.

- Brunauer-Emmett-Teller Method (BET Method)
- Iodine Number Method
- Methylene Blue Adsorption Method

The BET method involves the multilayer adsorption of gaseous molecules on the surface of adsorbent. The gases may be nitrogen, oxygen, argon or methane. This technique is better than others as the specific surface area of the solid surface calculated is of higher accuracy. But the experimental set up is tedious and needs special skills as well as specific instrument which are not available in our country at present.

Similarly, the iodine number method also correlates the surface area of adsorbent. Because of not general to all types of adsorbent, its reliability has been considered to be poor. Among these, the spectrophotometric determination of specific surface area from Methylene Blue Adsorption Method is the better one because of its simplicity, rapidity, easiness and reliability. And the chemical reagents are cheap and available in the market. The technique is easily performed in any ordinary laboratories.

In this method, small amount of activated carbon is added to the varying concentrations of methylene blue solution. The solutions are kept in mechanical shaker for 24 hours. The

resultant supernatant solution is pipetted out and the absorbance is taken at 660 nm wavelength. From the Langmuir adsorption isotherm graphs, the specific surface area can be determined[28, 29]. The specific surface area is calculated by the following equation

$$S_{MB} = \frac{N_g \times a_{MB} \times N \times 10^{-20}}{M} \quad \ldots\ldots\ldots \quad (1.4)$$

Where, S_{MB} is the specific surface area in 10^{-3} km^2/kg, N_g is the number of molecules of methylene blue adsorbed at the monolayer of the activated carbon in kg/kg (or $N_g = N_m$ x M), a_{MB} is the occupied surface area of one molecule of methylene blue =197.2 $Å^2$, N is Avogadro's number (6.023×10^{23}), M is the molecular weight of methylene blue (319.85 g/mol) and $\frac{N_g}{M}$ gives mmol/g which is equivalent to the Q_m of the Langmuir equation (vii).

1.4 Methods for the Determination of Lead (II) Ion

Several methods have been developed and reported in the literature, for the analysis of Lead in water. Among these some are expensive and time consuming while other are inexpensive, rapid and more effective. The AAS is the most sensitive and rapid technique[10].

The concentration of lead can be determined by flame technique of Atomic absorption Spectrophotometer which is operated by Air/Acetylene gas flow under secondary pressure 11.5-14.5 psi. Before the determination of unknown sample solution, the instrument is to be calibrated each and every time to obtain the calibration curve. With the help of this calibration curve and absorbance, the concentration of unknown solution can be determined. The λ_{max} for lead metal is 283.3 nm at slit width 1nm. For the determination of lead, the calibration curve is obtained by using the lead (II) solutions of concentrations 1, 5 and 10 mg/L. The sensitivity of AAS can be checked by 5mg/L of lead solution that gives the absorbance 0.2 at λ_{max} = 283.3 nm and slit width is 1nm. The instrumental detection limits for the determination of lead by flame and graphite tube atomizer are 0.01 mg/L and 0.06 µg/L respectively.

1.5 Adsorption Isotherm

Adsorption isotherm is a curve which relates the amount of adsorbate adsorbed per unit mass of adsorbent to the equilibrium concentration at constant temperature. Another definition, adsorption isotherm is a graphical representation of the amount of the adsorbate adsorbed per unit mass of the adsorbent as a function of the amount of the adsorbate left in bulk solution at equilibrium at constant temperature. Several models have been developed to describe the adsorption behavior like Langmuir isotherm model, Freundlich isotherm model, Dubinin-Radushkevich isotherm model, Temkin isotherm model, Flory–Huggins isotherm model and Hill isotherm model. Among them, Langmuir and Freundlich adsorption isotherms are the well-known models.

In 1918, Langmuir established the first quantitative model of adsorption. This model has been successfully applied for the adsorption of solute from a liquid solution, which involves active adsorbent sites, homogenous surface for adsorption with the formation of monolayer coverage and adsorption is independent of the occupation of neighboring sites[30]. Langmuir isotherm is used to estimate the maximum adsorption capacity corresponding to complete monolayer coverage on the adsorbent surface. Langmuir isotherm model is described by:

$$\mathrm{Q_e} = \frac{Q_m b C_e}{1 + bC_e} \qquad \cdots\cdots \qquad (1.5)$$

Where Q_e is the adsorption capacity in mg/g at equilibrium; C_e is the equilibrium concentration in mg/L; Q_m is the maximum adsorption capacity corresponding to complete monolayer coverage mg/g and b is the Langmuir adsorption equilibrium constant in L/mg. In order to establish the maximum adsorption capacity, the linear form of Langmuir adsorption isotherm is provided by the following equation:

$$\frac{\mathrm{C_e}}{\mathrm{Q_e}} = \frac{1}{Q_\mathrm{m}\mathrm{b}} + \frac{1}{Q_m} \cdot C_e \qquad \cdots\cdots \qquad (1.6)$$

A plot of C_e/Q_e against C_e gives a straight line with slope $1/Q_m$ and intercepts $1/Q_m b$ from which the value of Q_m and 'b' can be determined.

The essential features of the Langmuir isotherm can be expressed in terms of a dimensionless constant separation factor or equilibrium parameter (K_L), which is given by the relationship:

$$K_L = \frac{1}{1 + bC_i} \qquad \cdots\cdots \qquad (1.7)$$

Where, C_i is the initial concentration of the adsorbate (mgL^{-1}) and K_L indicates the shape of isotherm and nature of the adsorption process, ($K_L > 1$, unfavorable, $K_L=1$, linear, $0 < K_L < 1$ favorable, $K_L= 0$, irreversible). The value of K_L between 0 and 1 indicates that adsorption is favorable[31].

The adsorption data obtained can also be analyzed with Freundlich adsorption model. In 1906, Freundlich established relationship that describes the adsorption phenomenon[32]. The linear form of Freundlich isotherm is given by the equation.

$$Qe = K_F C_e^{1/n} \qquad \cdots\cdots \qquad (1.8)$$

Where, Q_e is the amount of adsorbate adsorbed per unit mass of adsorbent (mg/g), C_e is the equilibrium concentration of the adsorbate (mg/L); 'K_F' and 'n' are Freundlich equilibrium coefficient, which are considered to be the relative indicators of adsorption capacity and adsorption intensity. The logarithmic form of the Freundlich equation is given by:

$$\log Qe = \log K_F + \frac{1}{n} \log Ce \qquad \cdots\cdots \qquad (1.9)$$

When log Q_e is plotted against log C_e, a straight line is obtained with slope 1/n and intercept log K_F. From this plot, the value of 1/n and K_F can be determined. The value of 1/n between 0.1 and 1.0 indicates the favorable adsorption of heavy metal ions.

1.6 Adsorption Kinetics

The study of rate and mechanism of adsorption phenomenon is called adsorption kinetics. There are numerous adsorption kinetic models that are used to describe the uptake of adsorbate by different adsorbents. The pseudo-first order rate equation, the pseudo-second order rate equation and second order rate equation have been widely used for the description of adsorption kinetic model. The relationship between experimental data and the model predicted value is expressed by correlation coefficient. This helps in determining which reaction model better describes the adsorption of heavy metals onto

the adsorbent. A relatively high value of correlation coefficient (=1) indicates that the models successfully describes the kinetics of adsorption.

1.6.1 Pseudo-First Order Kinetic Model:

The pseudo-first order kinetic model is applicable for the reversible reaction with an equilibrium being established between liquid and solid phase. The linearized form of pseudo-first order rate equation [33] is generally expressed as:

$$\frac{dQ_t}{dt} = K_1(Qe - Qt) \quad \cdots\cdots \quad (1.10)$$

Where Q_e is the amount of metal adsorbed at equilibrium (mg/g) and Q_t is the amount of metal ion adsorbed at any time 't' (mg/g). Similarly, K_1 is the rate constant of pseudo-first order adsorption (per minute). After integration and applying boundary conditions, t=0 to t=t and $Q_t = 0$ to $Q_t = Q_t$, the linearized form of equation becomes,

$$\log(Qe - Qt) = \log Qe - \frac{K_1}{2.303}t \quad \cdots\cdots \quad (1.11)$$

The plot of log (Q_e-Q_t) versus 't' should give a straight line from which K_1 and Q_e can be determined from slopes and intercept of the plot respectively.

1.6.2 Pseudo-Second Order Kinetic Model:

The pseudo-second order reaction rate equation is used to study the kinetics of adsorption of heavy metal, which states that the rate of occupation of adsorption sites is proportional to the square of the number of unoccupied sites[34]. It is generally expressed as.

$$\frac{dQ_t}{dt} = K_2(Q_e - Q_t)^2 \quad \cdots\cdots \quad (1.12)$$

Where K_2 is the pseudo-second order rate constant (mg/g/min) and Q_t and Q_e are the amount of metal ion adsorbed at any time 't' and at equilibrium time respectively.

After integration and applying boundary conditions, t=0 to t=t and Q_t=0 to Q_t=Q_t, the equation becomes;

$$\frac{1}{Q_t} = \frac{1}{K_2 Q_e^2} + \frac{1}{Q_e}t \quad \cdots\cdots \quad (1.13)$$

If the initial adsorption rate is V_0 (mg/g min), then

$$V_0 = K_2 Q_e^2 \qquad \cdots\cdots \qquad (1.14)$$

The equation can be written as:

$$\frac{t}{Q_t} = \frac{1}{K_2 Q_e^2} + \frac{1}{Q_e} t \qquad \cdots\cdots \qquad (1.15)$$

Experimentally, the value of Q_e and K_2 can be determined from the linear plot of t/Q_t versus 't' with the slope and intercept of the plot respectively.

1.6.3 Intraparticle Diffusion Model

Intraparticle diffusion model is applied to gain insight into the mechanisms and rate controlling steps affecting the kinetics of adsorption. The kinetic experimental results are fitted to the following Weber-Morris equation[35].

$$\mathrm{Qt} = K_{id} t^{0.5} + \mathrm{C} \qquad \cdots\cdots \qquad (1.16)$$

Where C is the intercept and K_{id} (mg/g $\mathrm{min}^{0.5}$) is the intraparticle diffusion rate constant, which can be evaluated from the slope of the linear plot of Q_t versus $t^{0.5}$.The intercept of the plot reflects the boundary layer effect. The larger the intercept, the greater is the contribution of the surface sorption in the rate-controlling step. If the regression of Q_t versus $t^{0.5}$ is linear and passes through the origin and then intraparticle diffusion is the sole rate-limiting step. When the plots do not pass through the origin, this indicates some degree of boundary layer control and these further shows that the intraparticle diffusion is not the only rate-determining step but other kinetics models may also control the rate of adsorption.

1.7 Thermodynamic Studies

Thermodynamic consideration of adsorption process is necessary to conclude whether the process is spontaneous or not. The Gibbs free energy change (ΔG°) is a critical factor for determining the spontaneity of a process. The Langmuir constant b is related to free energy change of adsorption ΔG (kJ/mole) by the following relation[36].

$$\Delta G = -RT\ln(b) \quad \cdots\cdots \quad (1.17)$$

Where, R = Universal gas constant (8.314 $Jmol^{-1}K^{-1}$) and T = Temperature in Kelvin

Gibbs free energy indicates the degree of spontaneity of adsorption process. More negative value reflects greater energetically favorable process.

1.8 Error Analysis for Isotherm Studies

In case of single element isotherm studies, there is the need of error function to optimize the procedure in order to evaluate the fit of the isotherm to the experimental equilibrium data. There are several different error functions. The error functions are the sum of the squares of the errors, the hybrid fractional error function, Marquardt's percent standard deviation, the sum of the absolute errors and chi square test. The best fit among the isotherm models is given by the linear coefficient of determination (R^2) and non-linear Chi square (χ^2)[37]. In this study, the Chi-square test was performed for using the mathematical expression:

$$\chi^2 = \sum \frac{(Q_{e,cal} - Q_{e,exp})^2}{Q_{e,cal}} \quad \cdots\cdots \quad (1.18)$$

Where $Q_{e,calc}$ is the equilibrium adsorption capacity obtained by calculated from model (mg/g) and $Q_{e,exp}$ is the equilibrium adsorption capacity (mg/g) from the experimental data. The lower value of χ^2 suggest the best fit model.

1.9 Literature Review

Coal has been used as a fuel since at least early Greek and Roman times. The Greek philosopher Theophrastus, in his 4th century B.C treatise on stones, described a fossil substance used as a fuel. Coal cinders found in roman ruins in Britain show that coal was used during the Roman occupation of ca.50-450 A.D. Like petroleum and natural gas, coal is a fossil fuel. It is formed primarily from vegetation that flourished about 300 million years ago, when swamps covered much of the earth surface. As the vegetation grew and died, its remains sank into the swamp and later formed peat. Over millennia, layers of sediment and soil accumulated over the peat. A combination of geothermal heating and pressure from overlying deposits eventually formed carbon reach coal[11].

Coal is one of the most complex natural materials consisting of organic and inorganic constituents with various origins formed in sedimentary environment. Inorganic component constituent a small part of coal but most of the problem associated with coal is due to this fraction. The mineral matter of coal provides information about possible toxic trace elements. The analysis of Coal by various researchers reveal it contain 60-80 % carbon, 10-15 % sulphur by dry weight basis. The inorganic minerals present are quartz (majority), muscovite, calcite, dolomite, ankerite, hematite, gypsum, illite, kaolinite and pyrite. There is infinite variation based on coal origin, deposition and geology involved[38].

The Coal powered thermal power industries produce 750 million tons of CFA on the annual basis. India alone produces 112 million tons of CFA per annum as of 2012. This figure will grow as India, China, Africa and South America charges ahead in industrialization. The global recycling rate of CFA is 15%. Germany produces 40 million tons of CFA per annum[3, 39, 40]. Finland is highly industrialized country with high emphasis on innovation. The chemical industry in Finland is quite significant and combined with the fact that it is in situated in a cold region creates a huge demand for heat, electricity and power. Finland has a lot of Coal based power plant all over the country. The annual production of CFA is estimated to be 750,000 tons[41].

According to literature, four different type of Coal fly ash exists; anthracite, bituminous, subbituminous and lignite. The CFA generated from bituminous South African coal was found to contain 9.54 % CaO, 49.80 % SiO_2, 29.2 % Al_2O_3, 2.53 % Fe_2O_3, 1.49 % TiO_2 and 2.40 % MgO. The CFA typically comprises fine powders that are typically spherical, are either solid or hollow, and are mostly amorphous (glassy), although mullite and quartz

might coexist in crystalline phases. The glass phase plays important role in zeolite formation because of its high solubility in alkaline solution. It contains small amount of toxic heavy metals such as As, Mn, V and Pb but they are separated effectively during zeolitization. These metals exist in glass phase. Therefore they dissolve in alkaline solution and are therefore not incorporated into zeolites. The specific gravity of fly ash is 2.1-3.0; its specific surface area is 170-1000 m^2/kg[11].

Zeolites are extremely versatile materials. They are microporous aluminosilicates used especially as adsorbent and catalysts. It has wide range of applications in all sector of chemical industry in various forms. It can be used in powder, pellet, membrane thin films and other forms. The price of zeolite varies from 1000 Euros/ton to 20000 euros per ton based on the purity and applications. Hence it is evident that producing zeolites could bring higher economic benefits compared to other use of CFA[42]. Literature shows that zeolite-X has the chemical composition as shown in table below[10].

Table 1.2: Chemical composition of zeolite-X

component	**composition (%)**
SiO_2	38.7
Al_2O_3	20.9
CaO	8.1
Fe_2O_3	15.5
TiO_2	4.4
MgO	1.2
Na_2O	6.7
Carbon	3.0
K_2O	0.3
others	1.2

The word zeolite come from Greeks words “Zeo” and “lithos” meaning to “boiling” and “stones”. Zeolites were first discovered 250 years ago by Swedish mineralogist Cronsted. For 200 years these were only museum attractions[43]. It was not until experts realized that zeolites existed in large quantities in deposits that they gained real importance for various application. Their success in applications and unique properties led expert to seek for way

to produce them in laboratories. The laboratories were successful and that led to synthesis of tailor made zeolites for possible myriad range of properties and application. Until now Zeolites have been synthesized from pure chemicals but lately attempts have been made to produce zeolites from industrial wastes and other side streams. In nature about 40 different kinds of zeolites exists. Synthetic zeolite chemists continue to make new zeolites and until now about 130 different zeolites have been conceived. The first synthetic zeolites were (A, X, Y) and found wide spread applications[8]. The timeline for various zeolite syntheses with unique framework is given in **Table 1.3**.

Table 1.3: Milestone in Zeolite synthesis[43]

Year	**Event**
1930-1940	Pioneering work by Barrer et al in synthetic zeolite synthesis.
1949-1954	Discovery and synthesis of zeolite (A, X, Y).
1954	Commercialization of zeolite (A, X, Y).
1967-1969	Synthesis of high silica zeolites MFI and BEA.
1980	Specialized zeolites by secondary synthesis routes (dealumination, iso-morphous substitution etc).
1982-1986	Synthesis of alumino-phosphates (SAPO).
1983	Synthesis of titanium silicalites TS1.
1992	Mesoporous molecular sieves MCM41.
1994-1998	Nano crystalline zeolites made from pure chemicals.
1995-2015	Synthesis of zeolites from various industrial wastes and side streams.
2007-2008	Emergence of tailor made theoretical zeolites predicted by computational methods.
2009-2015	Emergence of zeolites made from industrial wastes and sidestreams. Development of waste to zeolite pilot and production facilities (Zeolite X, Y, P1 etc along with their variations).

Heavy metals is a collective term applied to a group of metals and metalloids with density greater than 5 g/cm, and include elements such as Cd, Cr, Hg, As, Mn and Pb. Literature

shows that removal of different heavy metals from aqueous can be done by ion exchange, precipitation, chelation, electrolytic recovery, Solvent extraction and Liquid membrane separation. These methods are not widely used due to their technical as well as economic constraints, so much attention has given to investigate the cost effective technique. Recently, use of waste materials for the heavy metal removal has been increasing because of their high metal uptake capacity and cost effective nature[44].

The removal of lead through adsorption by fly ash was investigated. Maximum adsorption of Pb (II) was 5.52 mg/g. It was found that the pseudo second order kinetic model provides the best description of fly ash adsorption behavior[45].

The activated carbon-zeolite X was used for the uptake of toxic metal ions. The relative selectivity for the various ions was $Pb^{2+} > Cu^{2+} > Cd^{2+} > Ni^{2+}$, with equilibrium uptake capacities of 2.65, 1.72, 1.44, 1.20 mmol/g respectively. The adsorption isotherm was good fit to the Langmuir isotherm. The overall reaction is pseudo-second order with rate constants of 0.14, 0.17, 0.21, 0.20 L.g/mmol min for the uptake of Pb^{2+}, Cu^{2+}, Cd^{2+}, Ni^{2+}, respectively[11].

Zeolite-P1 exhibited the highest adsorption capacity with a maximum value of about 1.29 mmol/g Pb (II) and had a strong affinity for Pb (II) ion. The metal ion selectivity of Na-P1 was determined as $Pb^{2+} > Cu^{2+} > Cd^{2+} > Zn^{2+}$ consisting with the decreasing order of the radius of hydrated metal ion. The adsorption isotherm of lead by Na-P1 fitted the Freundlich rather than the Langmuir isotherm[46].

The adsorptive separation of heavy metal on two species of waste seaweeds Ulva japonica and Porphyria yezoensis cross-linked with Calcium was studied. Maximum adsorption of Pb (II) was 0.77 mole/kg on Ulva japonica gel and in porphyria yezoensis gel Q_{max} was found to be 0.27 mol/kg for Pb (II)[47].

Activated carbon prepared from Coconut shell was used for the removal of Pb^{2+} from industrial waste water. The optimum adsorbent doses, stirring rate, and pH were found to be at 1g, 350 rpm and 6 respectively. Kinetics studies shows that pseudo second order model best describe the adsorption process. The activated carbon prepared from coconut shell can be efficiently used as low cost alternative for removal of metal ions[48].

The removal of Pb (II) and Cd (II) on to anaerobic granular biomass in aqueous solution over the pH range 4 to 4.5 demonstrated that the maximum adsorption capacity for Pb (II) and Cd (II) ions were 255 and 60 mg/g respectively. They also observed that the equilibrium data fitted well with Langmuir isotherm model[49].

The removal of Pb (II) by the adsorption on maize barn was investigated and the optimum pH for the removal was found to be 6 at 20 ºC. They obtained the experimental data fitted with Langmuir isotherm and pseudo-first order kinetic model was able to explain the adsorption process[50].

The removal of Lead (II) from aqueous solution on activated carbon and modified activated carbon prepared from dried water Hyacinth plant was carried out. In this work, potential of activated carbon stems and leaves (ACS, ACL) prepared from dried water Hyacinth steam and leaves (DS, DL) by chemical activation with phosphoric acid (1:3) and modified activated carbon stem and leaves (MACS, MACL) with nitric acid (1:1) for the removal of lead from aqueous solution was investigated. The maximum adsorption capacity of lead at pH 5 were in the order MACS (175.63 mg/g) > MACL (164.56 mg/g) > DS (90.50 mg/g) >DL (66.60 mg/g) > ACS (36.00 mg/g) > ACL (33.40 mg/g). The results showed that the experimental data fitted well to the Langmuir model and follow pseudo second order kinetics. The thermodynamic study reveals that the adsorption was spontaneous and endothermic process[51].

Lentil husk is an agricultural waste which was found to be promising low cost adsorbent for removal of Pb (II). The adsorption process was at optimized at pH 5.0 and temperature 30 ºC with an initial Pb (II) ion concentration of 250 mg/L. Adsorption process was well explained by Langmuir isotherm model with the maximum lead removal capacity 81.43 mg/g. Kinetics study showed that the adsorption follows pseudo-second-order rate model with rate constant 0.225 g/mg for 20 mg/L solution[52].

Activated carbon was prepared from the cones of the European Black pine and used as adsorbent for the removal of Pb (II) ions from aqueous solutions. The effect of pH, initial concentration of lead (II) ions, contact time, and adsorbent dosage on the adsorption was studied in batch experiments. Equilibrium data were best fitted to the Langmuir isotherm

with maximum adsorption capacity of 27.53 mg/g. The kinetic data were found to follow closely the pseudo-second-order model[18].

1.10 Statement of the Problems

The combustion of huge amount of coal leading to the generation of coal combustion byproducts (CCB). Consequently it leads to problems due to the limited land fill sites for the disposal of CCB generated. Another problem arises due to the different industrial effluents containing toxic metal ion that are directly passed into water sources without any treatment. Toxic metal ions can bio accumulates in the body and in the food chain that lead to the chronic nature of their toxicity. Some problems commonly faced on removal of toxic metal ions in water are as follows:

- Though, different physio-chemical methods are available for toxic metals ions removal, but, they are highly expensive, less effective and results in generation of toxic sludge.
- Though, commercial activated carbon is available for toxic metal ions removal but it is very expensive.
- Toxic metal ions removal filters are commercially available but is beyond capacity of developing country like Nepal.

1.11 Limitations of the Study

Due to the lack of facilities to trace out what type of zeolite was found, it was difficult to categorize the type of zeolite in this study. Further, due to not having the facilities of Scanning Electron Microscope, the exact shape of zeolitic material synthesized in this study was not mentioned.

1.12 Objectives of the study

Our country is facing with the significant challenge of safely managing several million tons of coal fly ash each year. These waste materials pose a potential threat to public health, safety and the environment.

1.12.1 General objectives

The goal of the present research work was to prepare a cost effective adsorbent from Coal Fly ash and to investigate the adsorption capacity of adsorbent in aqueous solution by using AAS (AA-7000, Shimadzu, Japan).

1.12.2 Specific objectives

The specific objectives of the present work are:

- Determination of the suitability of Nepalese CFA for synthesis of activated carbon-zeolite which can be used as adsorbent for waste water treatment.
- Characterization of the Coal Fly ash and final product i.e. activated carbon-zeolite using XRD, FTIR.
- Determination of the specific surface area of activated carbon-zeolite by using methylene blue adsorption method.
- Investigation of the effect of pH, initial concentration and reaction time of adsorption process.

CHAPTER 2

EXPERIMENTAL

All the experiments were performed in batch mode by using activated carbon zeolite composite prepared from coal fly ash fused with Sodium hydroxide. All the chemicals used for this dissertation work were of LR/AR grades and were used without further purification.

2.1 Preparation of Reagents

Preparation of methylene blue solution

The methylene blue (AR Grade, Qualigens Fine Chemicals, India) was weighed out accurately (0.250 g) in weighing balance (264, OHAUS, USA) and transferred to 500 ml volumetric flask. It was then dissolved with distilled water and marked up to the level with the same water. The solution thus prepared was stoke solution.

The appropriate volume of stock solution was taken to get the working methylene blue solutions of required concentration by dilution method.

Preparation of stock solution of Pb (II) solution

Lead Nitrate (1.598 g) was dissolved in distilled water. It was shaken and then 5 mL of concentrated HNO_3 was added and diluted with distilled water up to the mark in 1000mL volumetric flask. The obtained stock solution was used for working solution preparation required for each experiment.

1 ppm of Lead = 1 mg/L

1000 ppm of Lead =1000 mg/L

207.21 g of Lead is present 331.21 g of $Pb(NO_3)_2$

1 g of Lead is present in (331.21/207.21=1.598 g) of $Pb(NO_3)_2$

1000 mL of 1000 ppm Lead solution =1000 g of Lead

1 mL of 1000 ppm Lead solution =1000 μg of Lead

Preparation of working Lead (II) solution

Standard Lead solutions of required concentration were prepared by appropriate dilution of stock Lead solution. First 250 mg/L of Lead (II) solution was prepared from 1000 mg/L stock solution. From 250 mg/L of Lead (II) solution required lower concentrations were prepared by appropriate dilutions.

Preparation of 0.1 M NaOH Solution

About 1 g NaOH was dissolved in 250 mL V.F and diluted up to mark.

Preparation of 0.1 M HCl Solution

0.1 M HCl was prepared in 250 mL V.F by dilution of Conc.HCl.

Buffer solution

Buffer solution of pH 4, 7 and 9, employed for the calibration of pH meter were prepared by dissolving the respective buffer tablet in distilled water using 100 ml volumetric flask.

2.2 Preparation of Activated Carbon-Zeolite composite from Coal Fly Ash

Synthesis of activated carbon-zeolite

For the synthesis of zeolite, CFA was obtained from Uma-Maheshwor brick factory of Kathmandu valley. This CFA will be ground manually to obtain fine powder form by using mortar and pestle. It was sieved with a Tyler sieve of 75 micron mesh to obtain fine particles. The CFA was mixed with NaOH with varying mass ratio 1:2 and fired at 650 ºC for 1 h in a N_2 atmosphere in a tubular furnace (F21130-33, Thermolyne, USA). After the NaOH treatment, the mixture was ground and suspended in 12 ml deionized water in order to maintain NaOH concentration of 4M. The slurry was sealed in a microwave grade bottle and heated in a furnace at 80 ºC for 24 hrs. Then, the sample was washed several times using deionized water, dried at 50 ºC overnight, and then collected for characterization.

The schematic diagram of the pyrolysis of coal fly ash is shown in **Fig. 2.1**. The technique is environment friendly since the gas is passed from one side of the tube and other side contains the outlet of black smoke dipped into water trough. The tube, containing coal fly ash, is placed inside the furnace heated accordance to the need using

temperature controller. Atmosphere inside the tube can be changed as per the requirements. This can be done by passing nitrogen gas.

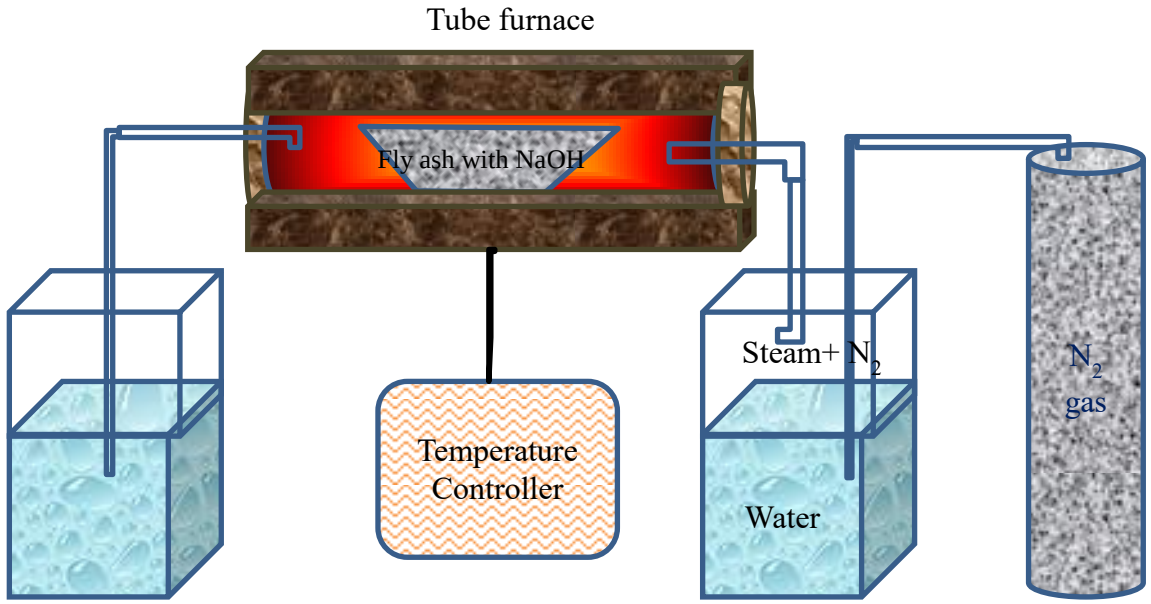

Fig. 2.1: Schematic diagram for the pyrolysis of coal fly ash

2.3 Adsorption Studies

Preparation of calibration curve for methylene blue solution

For preparation of calibration curve, at first the maximum absorbance was designed. Here it was done by preparing 5 mg/L solution of methylene blue. The absorbance was measured against wavelength ranging from 600 to 690 nm using Spectrophotometer (2306, Electronics, India). The maximum absorbance (λ_{max}) obtained, here was at 660 nm. After that the methylene blue solutions of 1, 2, 3, 4, 5, 6, 7, 8, 9 and 10 mg/L were prepared in 25 mL volumetric flasks. The absorbance of all the solutions was taken at 660 nm wavelength. A plot of absorbance versus concentration thus gave a calibration curve for methylene blue solution.

Determination of specific surface area of the activated carbon-zeolite

To determine the specific surface area of the activated carbon-zeolite, the Langmuir adsorption isotherm model was used. For this, 20 mg of activated carbon-zeolite was

weighed out accurately and transferred to 25 mL conical flask containing varying concentrations of methylene blue solutions (25-100 mg/L)

The solutions were shaken for 4 continuous hours in an orbital shaker (AI-153, Accumax, India). It was then allowed to rest for half an hour. Doing so the carbon settled down and the supernatant solution was pipetted out. The absorbance of the resultant solution was taken at 660 nm wavelength. From the Langmuir adsorption isotherm, Q_m value was calculated. And using the formula of specific surface area (equation **1.4)**, the specific surface area of the activated carbon-zeolite was determined.

Preparation of calibration curve of Pb (II) ion

Lead solution containing 1.0, 5.0 and 10.0 mg/L and blank solution were prepared in 25 mL volumetric flask. The absorbance of each solution was measured at 665 nm against blank solution with the help of AAS. A plot of absorbance versus concentration of Lead (II) was made.

Effect of pH

For the pH studies of Pb (II) adsorption, the initial concentration and volume of solution taken were 25 mg/L and 30 ml respectively. The solutions were taken in 100 ml beaker and the pH of the solutions were adjusted from 2 to 8 using appropriate strength of NaOH and HCl solutions by the help of pH meter (54/A-3, Accumax, India). To each beaker, 20 mg of the zeolite activated carbon composite adsorbent was added and then shaken in Mechanical shaker for 24 hours at a speed of 150 rpm. After shaking, each solution was filtered immediately using Whatman 41 filter paper and the equilibrium pH of the filtrate was noted. The filtrates were analyzed to determine the equilibrium concentration of Lead. With the help of initial and equilibrium concentrations, the percentage adsorption of Lead at each pH was determined. Thus, the optimum pH for the adsorption of Lead was evaluated.

Adsorption Isotherm Studies

The effect of Lead concentrations on the adsorption was studied under optimum pH. The adsorption isotherm study was done with different initial concentrations of Pb (II) ion ranging from 25 to 600 mg/L with 20 mg of zeolite activated carbon composite adsorbent. The solution was shaken in a mechanical shaker for 24 hours at speed of 150 rpm. The

equilibrium concentration of Lead was determined by Atomic adsorption spectrometer (AAS). Here, the two models had been tested to study the adsorption isotherm study.

Kinetic Studies

The adsorption kinetics experiments were performed at corresponding optimum pH for Pb (II) ion by equilibrating. For the study of kinetics behavior, 30 mL of 25 ppm Lead solutions in 50 mL Erlenmeyer flask containing 20 mg of zeolite activated carbon were used. These flasks were shaken for different length of time 5 to 150 minutes, in a mechanical shaker for 24 hrs at speed of 150 rpm. The kinetics were investigated by taking out flasks at desired period of contact time and immediately filtered through What-man 41 filter paper to obtain filtrates and the concentrations in the filtrates were determined by Atomic Absorption Spectroscopy (AAS). The data was tested with pseudo-first order and pseudo-second order kinetics models.

2.4 X-ray Diffraction (XRD) Analysis

The sample, without any adsorption was analyzed for the phase detection using X-ray Diffractometer with monochromatic CuKα radiation (D2 Phaser Diffractometer, Bruker, Germany) at Nepal Academy of Science and Technology (NAST). The sample was scanned at 2θ from 10 to 80º. The XRD was done to determine the phases of activated carbon-zeolite and coal fly ash.

2.5 FTIR Analysis

The sample, without any adsorption were analyzed by using Fourier transform infrared spectroscopy (IR Tracer 100, Shimadzu, Japan) at Central Department of Chemistry, Tribhuvan University for the functional groups identification in activated carbon-zeolite composite.

CHAPTER 3

RESULTS AND DISCUSSION

3.1 X-ray Diffraction (XRD) Analysis

The physical properties of activated-carbon zeolite composite are fundamental parameters for the contaminant adsorption effectiveness. It has been shown for activated carbon zeolite that high specific area contributes to high adsorption capacity and favorable pore structure facilities fast mass transfer or intra-particle diffusion. The XRD patterns of the coal fly ash and its NaOH treated sample are show in figure below. XRD is used to determine the crystallinity of zeolite.

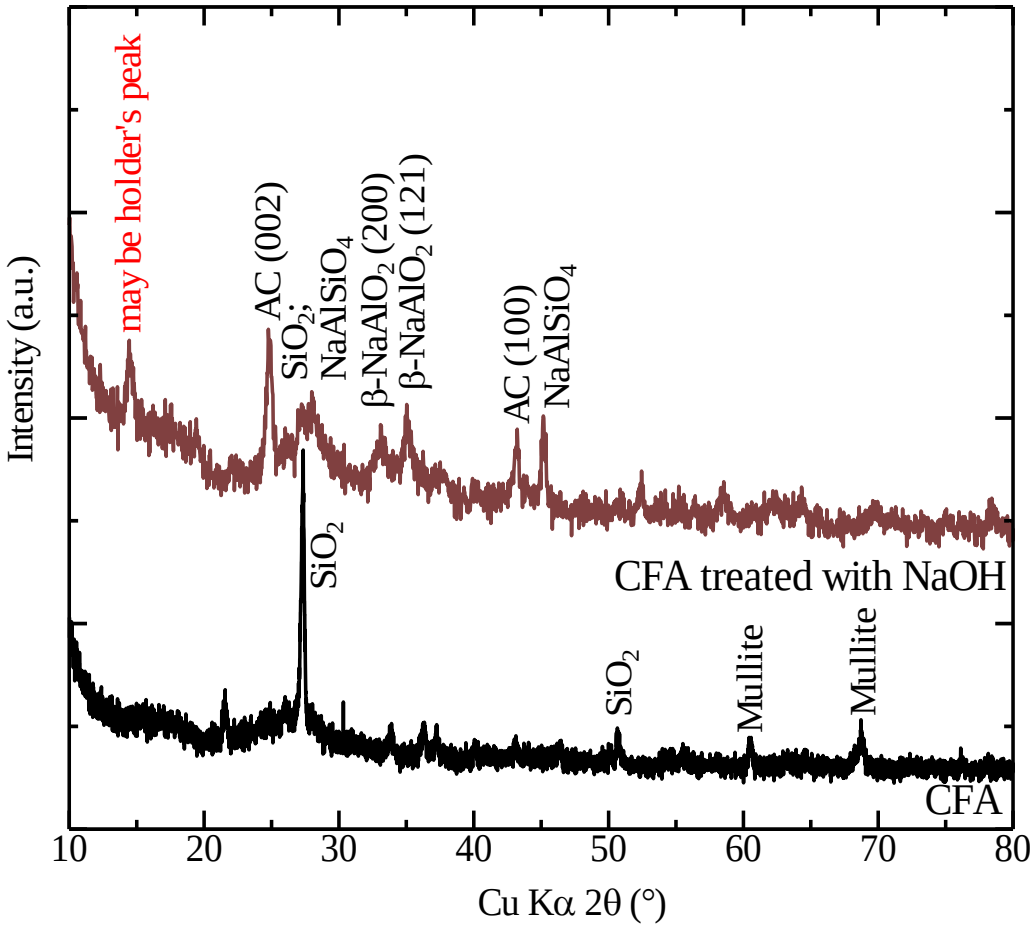

Fig. 3.1: X-Ray diffraction patterns of coal fly ash (CFA) and its NaOH treated samples

Coal fly ash normally contains SiO_2 and mullite ($3Al_2O_3{\cdot}2SiO_2$) phases. The major components SiO_2 and mullite ($3Al_2O_3{\cdot}2SiO_2$) along with unburned carbon were activated

by NaOH fusion treatment at 650 °C in a N_2 atmosphere. It was the target to synthesize zeolite sample from coal fly ash but in absence of autoclave the exact product was not obtained. Due to the absence of the calibration of XRD instrument in order to get exact peaks below 2θ value of 10° and the exact characterization of XRD peaks, it is difficult to say whether the any type of zeolite was formed or not. But from XRD pattern it can be seen that NaOH was reacted with aluminosilicate available in coal fly ash and thus $NaAlO_2$ (2θ = 33° and 35°) as well as $NaAlSiO_4$ (2θ = 26-29° and 45°) were formed. The presence of activated carbon is also seen in the XRD pattern.

3.2 FTIR Analysis

The FTIR spectrum of activated carbon zeolite is shown in **Fig. 3.2**.

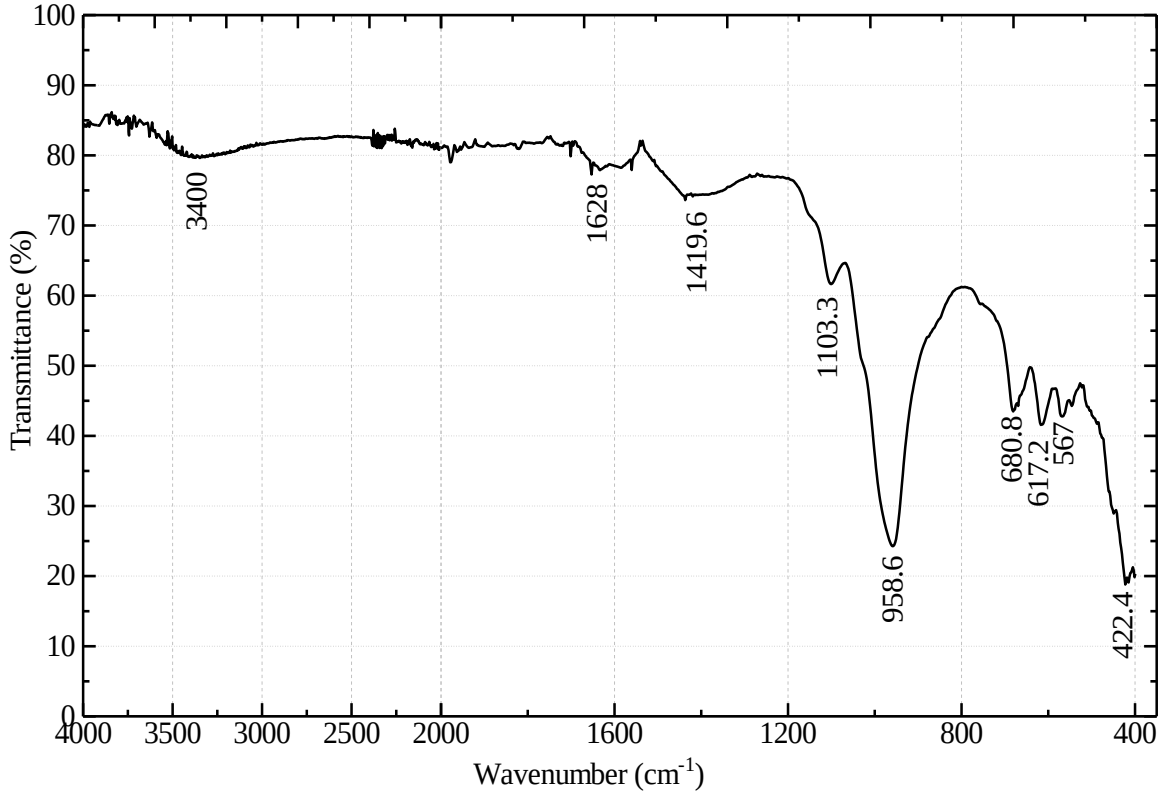

Fig. 3.2: FTIR spectrum of NaOH treated with coal fly ash sample

The FTIR spectra were obtained to understand the nature of functional group present in activated carbon zeolite sample. It indicates weak and broad bands in the region of 4000-400 cm^{-1}. The broader bands in the wave number region at 3400 cm^{-1} corresponds to the symmetric and asymmetric stretching vibration of OH group. The peak appearing at 2000cm^{-1} may be of residual water.

The peak at 1628 cm^{-1} is due to symmetric stretching of the C=O groups. The peak at 1419.6 corresponds to aromatic carbon–carbon (C=C) stretching vibration. The peak at 958.6 cm^{-1} corresponds to the asymmetric stretching vibrations of Si-O-Si bonds or Al-O-Al bonds or Si-O-Al bonds. The peak at 680.8 cm^{-1} corresponds to the symmetric vibration of internal tetrahedral (Al-O-Al bonds or Si-O-Si bonds). Band at 567 cm^{-1} can be ascribed to double ring mode of external linkage of zeolite framework. The band at about 422.4 cm^{-1} can be assigned to O-Si-O (or O-Al-O) bending vibration in internal tetrahedral[53].

3.3 Determination of λ_{max} of the Methylene Blue Solution

The absorbance of methylene blue with the variation of wavelength is shown in **Fig. 3.3** (data taken from **Table A** of **Appendices**). As shown in **Fig**. **3.3**, the maximum absorbance was obtained at 660 nm which is in trend with the previous report[29].

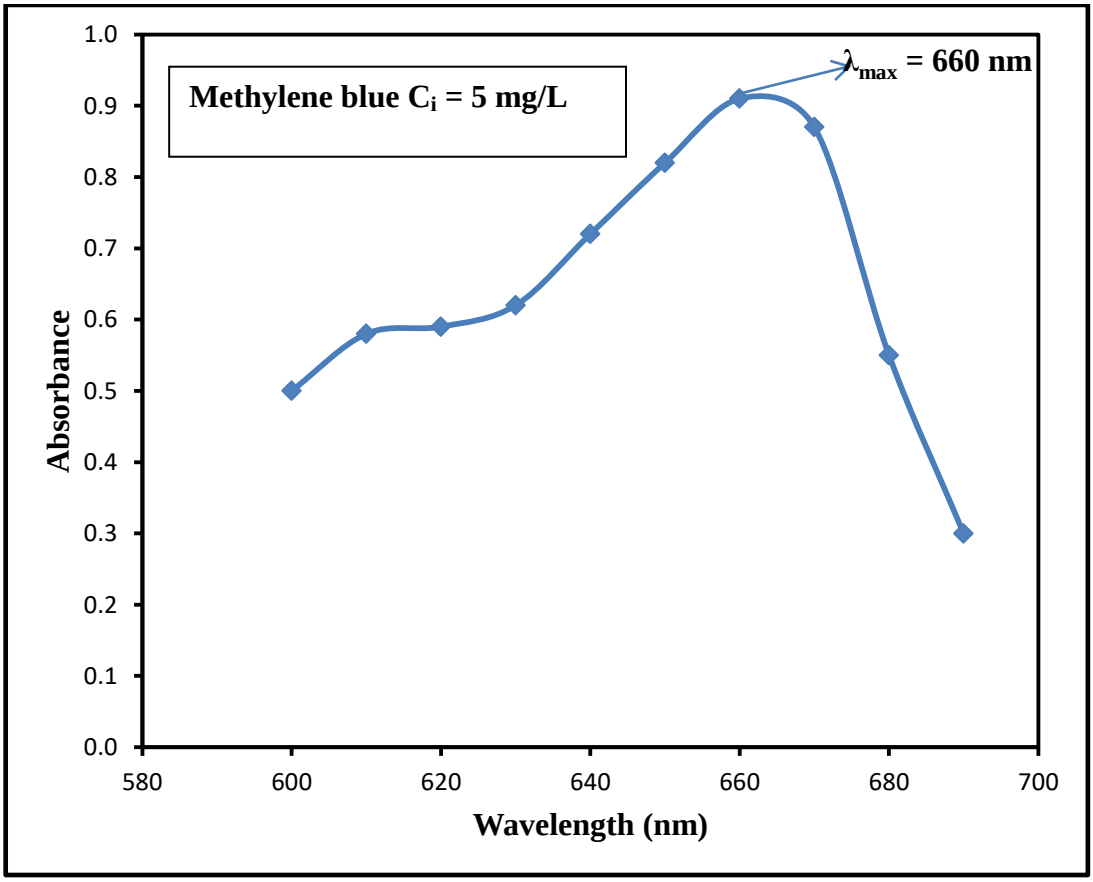

Fig. 3.3: A plot of absorbance as a function of wavelength at constant concentration of 5 mg/L methylene blue solution.

3.4 Calibration Curve of the Methylene Blue Solution

The calibration curve of the methylene blue solution is shown in **Fig. 3.4 (**data taken from **Table B** of the **Appendics**). It shows that the linear relationship between the absorbance and the concentration up to 10 mg/L and thus follows the Beers Lambert Law. For higher concentration of methylene blue solution further dilution required.

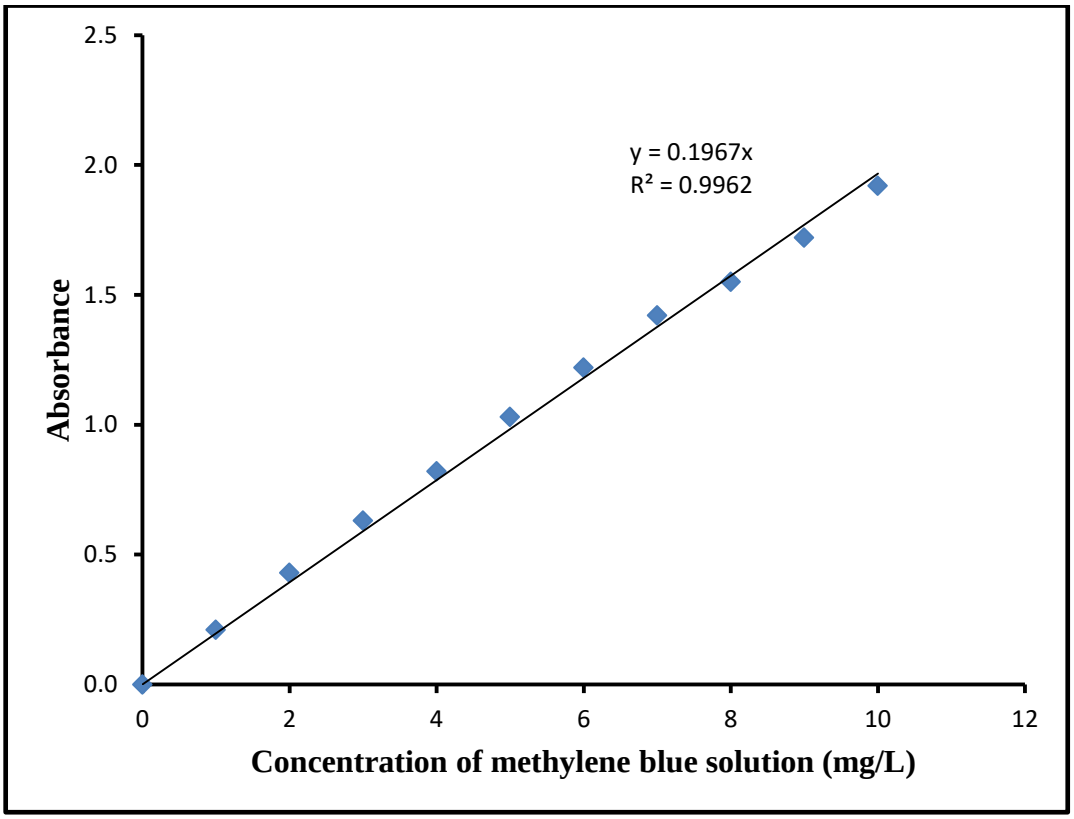

Fig. 3.4: A plot of absorbance as the function of concentration of methylene blue solution.

3.5 Specific Surface Area Determination

To determine the specific surface area, the linearized Langmuir curve is to be drawn. The curve for activated carbon-zeolite is shown in **Fig. 3.5** (data taken from **Table C** of **Appendices**) and the corresponding Langmuir parameters are shown in **Table 3.1.** The specific surface area of the activated carbon-zeolite was calculated with the help of slopes obtained from the curves.

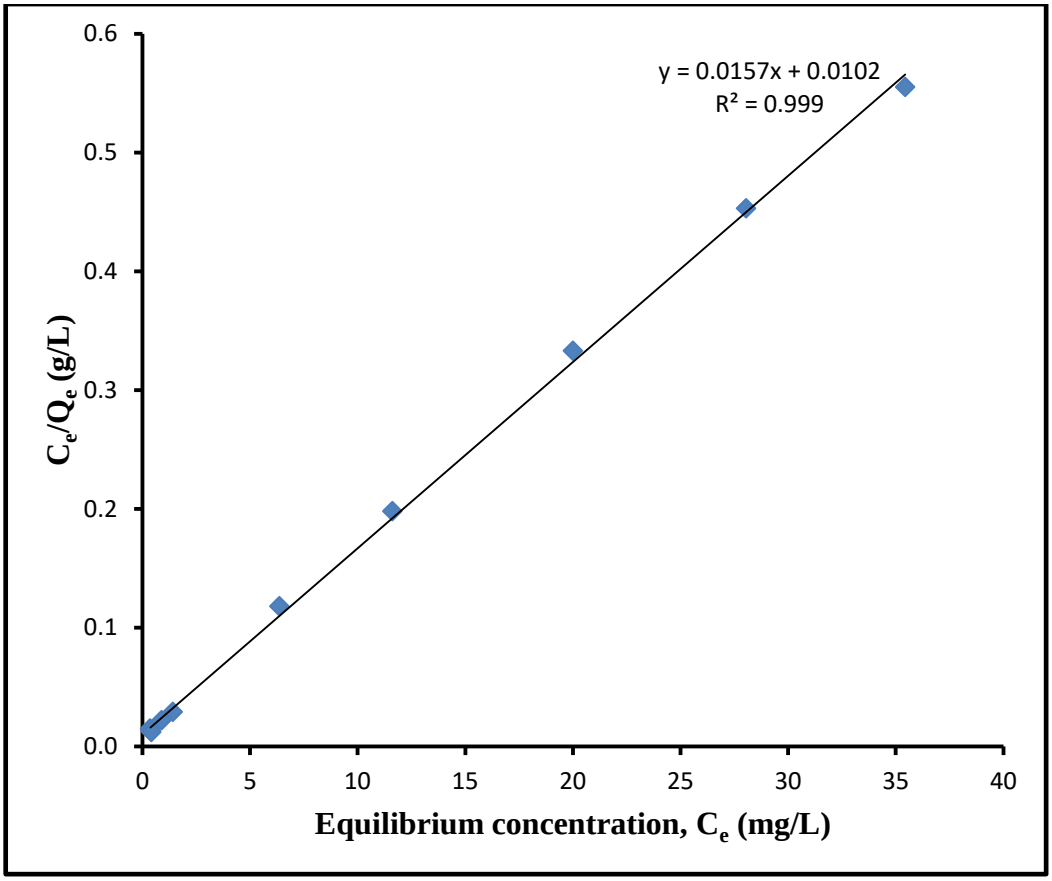

Fig. 3.5: A plot of C_e/Q_e versus C_e of activated carbon-zeolite

Table 3.1: Langmuir parameters for adsorption of methylene blue

Type	**Langmuir parameters**		
	Q_m (mg/g)	**b (L/mg)**	**R^2**
Activated carbon zeolite	63.69	1.53	0.999

The specific surface area of activated carbon-zeolite was found to be 241 m^2/g.

3.6 Calibration Curve for the Lead (II) ion Solution

The calibration curve of the Lead (II) solution is shown in **Fig. 3.6** (data taken from **Table D** of **Appendices**), which shows that the plot is linear and obey Beer-Lamberts Law between the absorbance and the concentration up to 10 ppm.

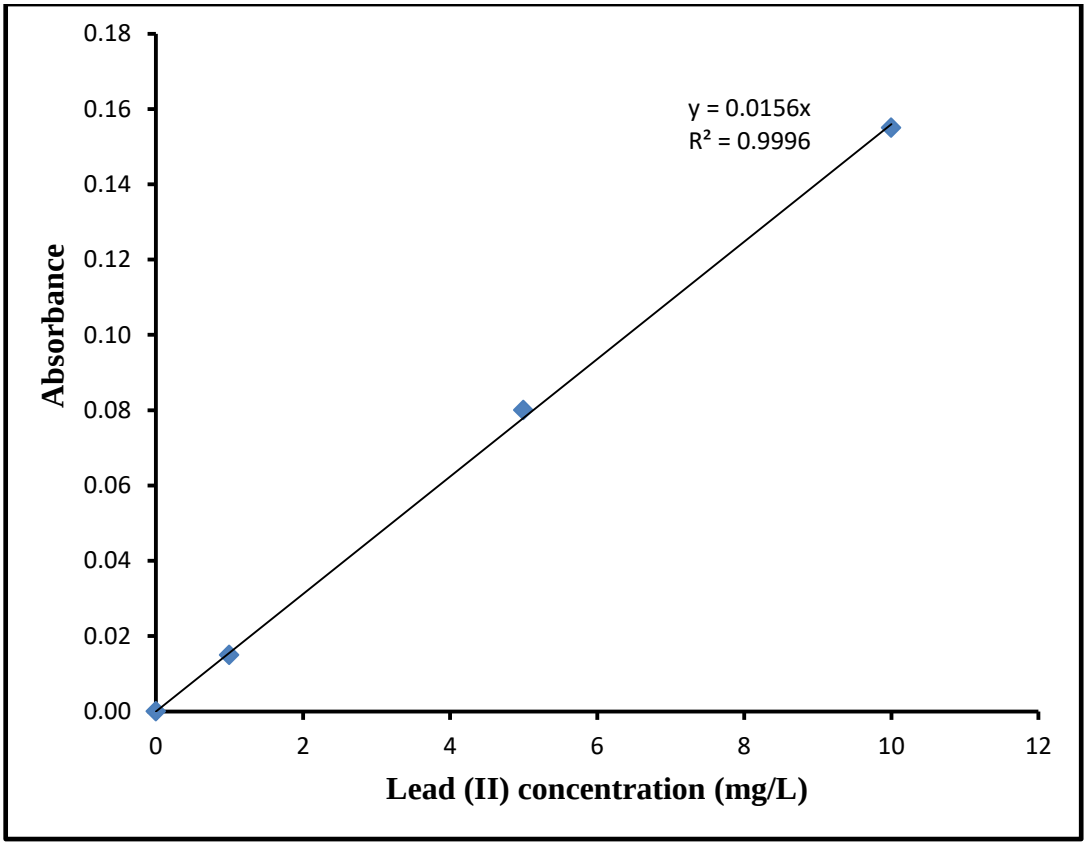

Fig. 3.6: A plot of absorbance as the function of concentration of Lead (II) ion solution

3.7 Effect of pH

The effect of pH on adsorption process is illustrated in **Fig. 3.7 (**data taken from **Table E** of **Appendices**) which shows the relationship between adsorption (%) and the initial pH in the adsorption of Lead (II) ion onto activated carbon zeolite at the initial concentration of 25 ppm (mg/L). In the study of Lead (II) ion was adsorbed by varying the pH from 2 to 8. The maximum adsorption percentage was found at pH 6, which was 94.00 %. Hence the pH 6 was designed as optimum pH. The removal efficiency was poor in acidic environment due to the instability of zeolite framework at lower pH. At low pH, some functional groups may be positively charged and their interaction with metal ion can be hindered significantly. So the adsorption of Pb (II) ion onto activated carbon zeolite at lower pH decreases.

In other word low degree of adsorption at low pH is that, H^+ ions concentration is high and therefore protons can compete with Pb (II) in forming a bond with the surface active sites. These bonded active sites become saturated with H^+ and was inaccessible to Pb (II) ions. In addition when pH increases, there is decrease in positive surface charge because

the deprotonation of the adsorbent functional groups occur which results in lower electrostatics repulsion between the positively charged metal ions and the surface of zeolite favoring adsorption. i.e with increase in pH of the solution, charges on the surface of zeolite becomes negative. There by leading to an attraction forces between Pb (II) and zeolite, enhancing adsorption. Hence an increase in adsorption of Pb (II) from solution onto activated carbon zeolite.

The maximum removal of Lead (II) was occurred at pH 6 for activated carbon-zeolite. This is also clear from **Fig. 3.7** which shows there is decrease in actual concentration of Pb (II) at pH greater than 6 due to precipitation of lead (II) as hydroxide form.

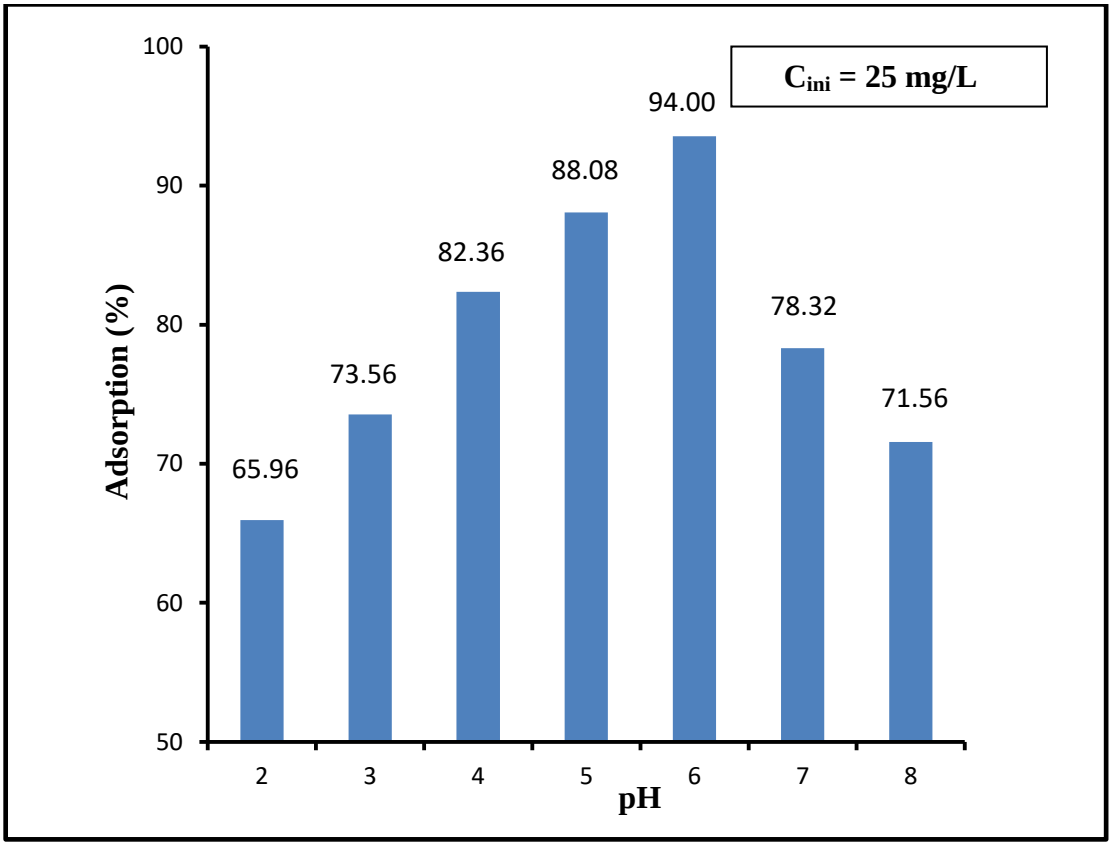

Fig. 3.7: Adsorption of Lead (II) with the variation of pH of the solution.

3.8 Adsorption of Lead (II)

The adsorption study of Lead (II) onto zeolite activated carbon was done by optimizing the pH at 6 and varying the concentration of Lead (II) from 25-600 mg/L. The linearized Langmuir and Freundlich curves (data taken from **Table F** of **Appendices)** are shown in **Fig. 3.8** and **3.9** respectively. The corresponding Langmuir and Freundlich parameters are shown in **Table 3.2.**

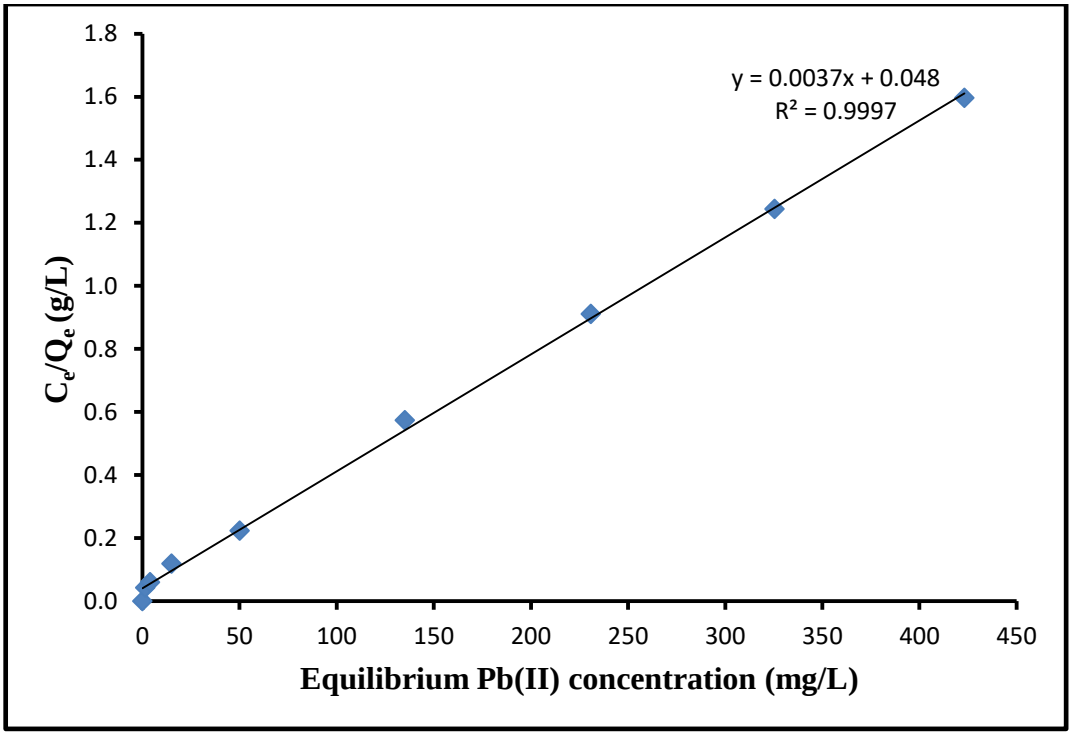

Fig. 3.8: The linearized Langmuir curve for the adsorption of Lead (II) onto activated carbon zeolite.

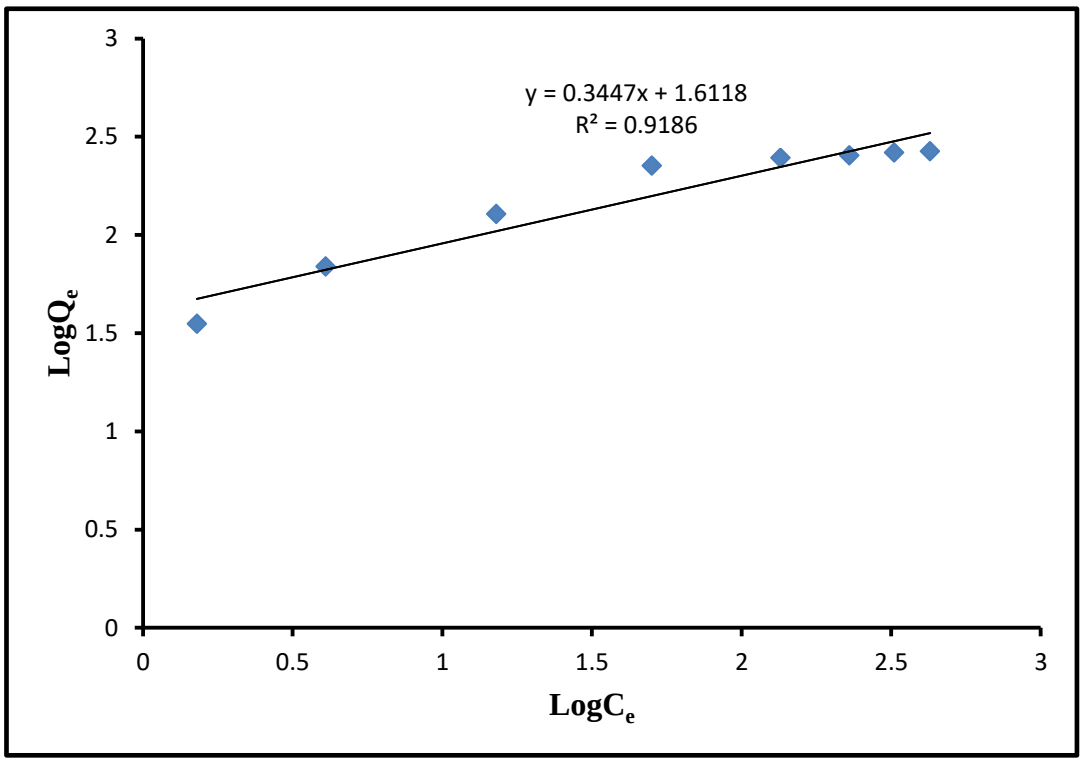

Fig. 3.9: The linearized Freundlich curve for the adsorption of Pb (II) onto activated carbon zeolite

Table 3.2: Parameters of Langmuir and Freundlich constants

Langmuir Model					Freundlich model			
Q_{max} (mg/g)	b (L/mg)	R^2	ΔG (kJ/mole)	χ^2	K_F (L/g)	n	R^2	χ^2
270.27	0.077	0.9997	-24.00	0.880	40.93	2.90	0.9186	7.163

The Pb (II) adsorption isotherm curve is shown in **Fig. 3.8 and 3.9.** The Langmuir and Freundlich models were used to fit the experimental data which was shown in the **Fig. 3.10.** From the **Table 3.2**, the value of ΔG was calculated and found to be -24.00 kJ/mole. The negative value of free energy (ΔG) in adsorption process reveals the spontaneous nature and feasibility of the adsorption process for the adsorption of Pb (II) onto activated carbon-zeolite. The value of ΔG confirms the adsorption process is favored by physio-chemical adsorption. The above table shows the value of n is 2.90.

The correlation coefficients of Langmuir and Freundlich isotherm are 0.9997 and 0.9186 respectively. Since the R^2 of Langmuir model is greater than that of Freundlich, so the adsorption of Pb (II) ion onto activated carbon zeolite was monolayer and involved the adsorption on homogeneous active surfaces. This implies that the experimental data fitted well to the Langmuir model. The Langmuir adsorption is of monolayer adsorption model and metal ions are taken up independently on single type of binding site in such a way that the uptake of first metal ion does not affects the adsorption of second metal ion. The Q_m value obtained from Langmuir Model was found to be 270.27 mg/g. The value of χ^2 for the Langmuir model is smaller than that of the Freundlich model which concludes that adsorption of Lead (II) on activated carbon zeolite follows the Langmuir adsorption isotherm. The corresponding K_L values obtained from **Table 3.3** are found to be between 0 and 1 which is in agreement with the favorable adsorption.

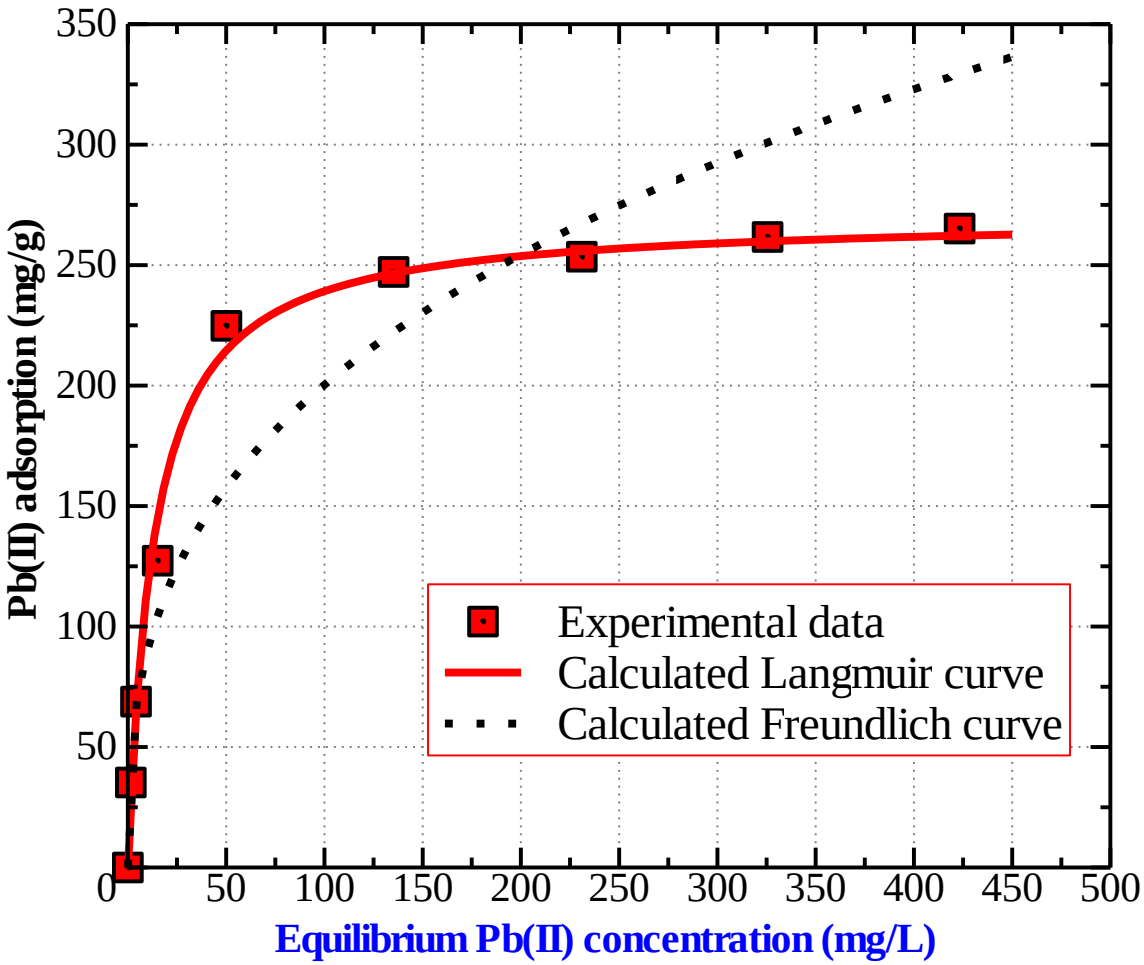

Fig. 3.10: The adsorption isotherm of Pb (II) onto activated carbon-zeolite

Table 3.3: Determination of Equilibrium parameters from Langmuir Isotherm

Initial concentration, C_i (mg/L)	**b (L/mg)**	**$1+bC_i$**	**K_L**
25	0.077	02.92	0.342
50	0.077	04.85	0.206
100	0.077	08.70	0.114
200	0.077	16.40	0.060
300	0.077	24.10	0.041
400	0.077	31.80	0.031
500	0.077	39.50	0.025
600	0.077	47.20	0.021

The value of K_L lies between 0 and 1 which indicates that adsorption is favorable**.**

3.9 Kinetics Studies

The study of adsorption kinetics describes the solute uptake and the time required for the adsorbate uptake at the solid-solution interface. The kinetics mechanism that controls the adsorption process onto activated carbon zeolite was evaluated by using pseudo-first order and the pseudo-second order kinetics model. The effect of contact time of the two models pseudo-first order and pseudo second order model were studied and their plot are shown in **Figs. 3.11 and 3.12 respectively** (data taken from **Table G of Appendices**). The rate of reaction as well as the maximum adsorption capacities obtained from the slopes and intercepts of **Figs. 3.11** and **3.12** are shown in **Table 3.4**. The correlation coefficient values of pseudo-first order and pseudo-second order models are 0.9397 and 0.9984 respectively showed that the kinetics of Pb (II) onto activated carbon zeolite followed pseudo-second order kinetics.

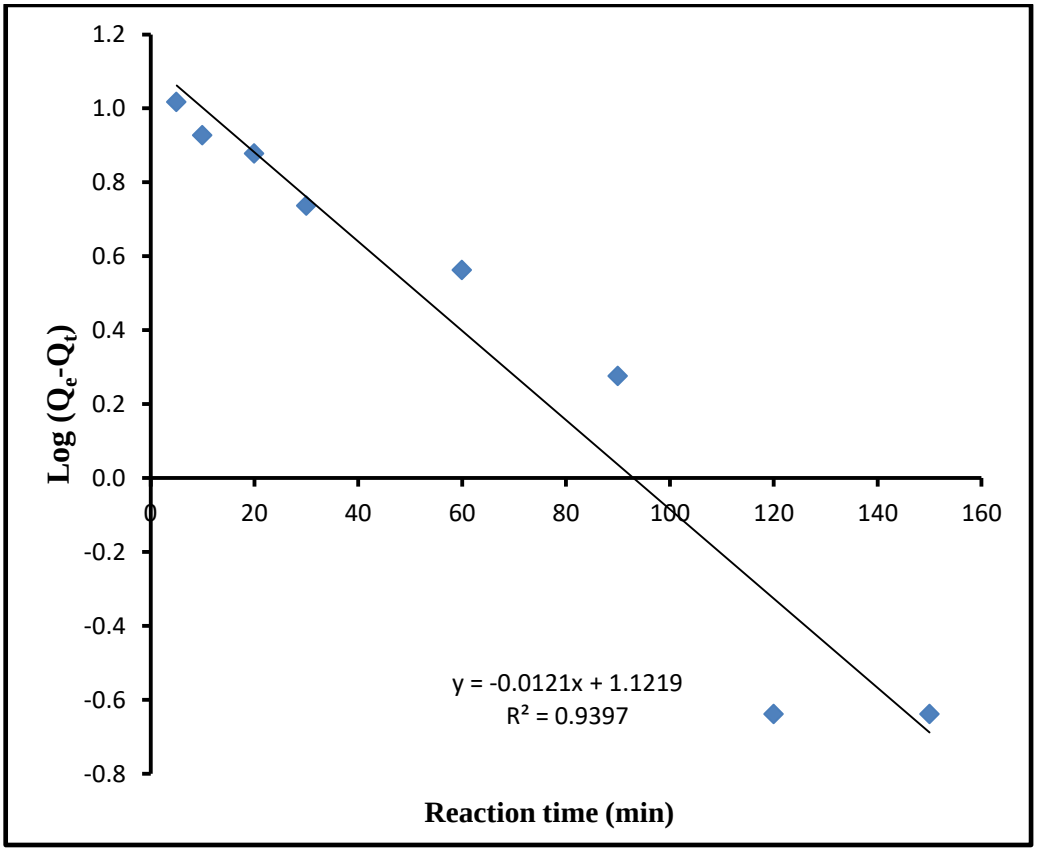

Fig. 3.11: Pseudo first order kinetics model for adsorption of Pb (II) ion onto activated carbon zeolite.

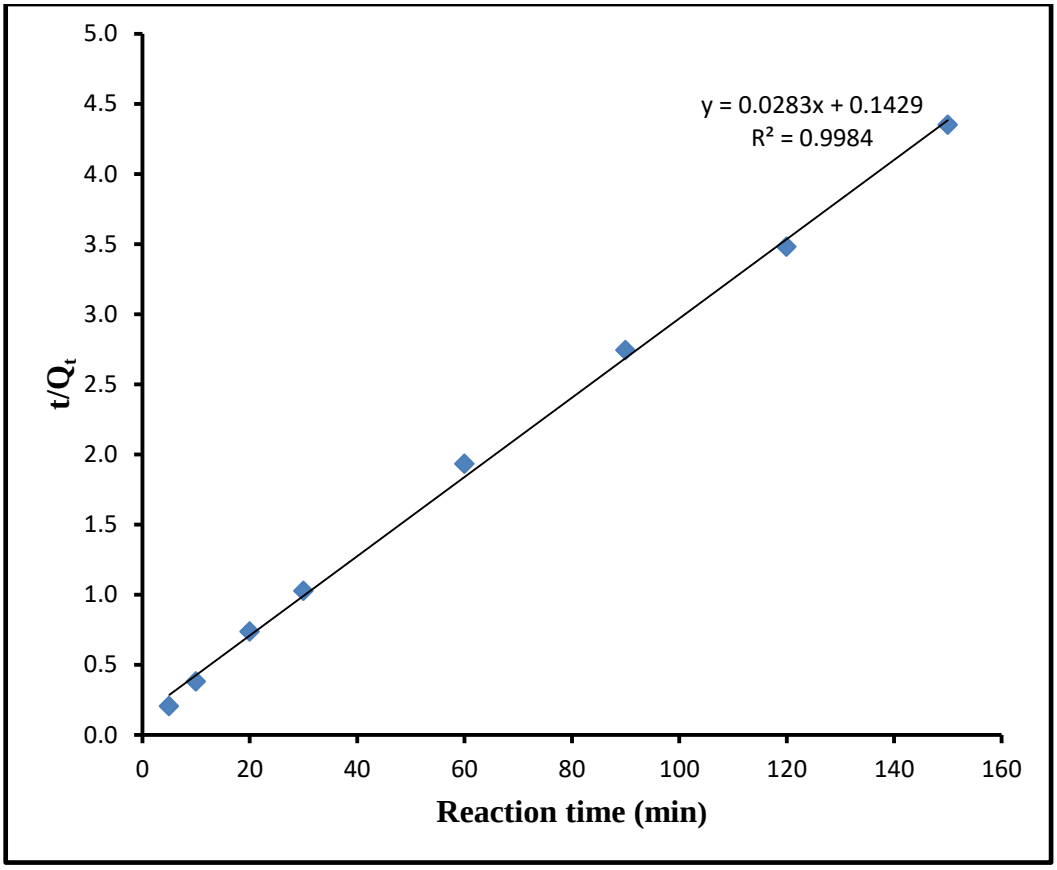

Fig. 3.12: Pseudo second order kinetics model for the adsorption of Pb (II) ion onto activated carbon zeolite

Table 3.4: Kinetics parameters of Pb (II) adsorption on activated carbon zeolite

Pseudo first order model			**Pseudo second order model**		
Q_e (mg/g)	K_1 (min^{-1})	R^2	Q_e (mg/g)	K_2 (g/mg.min)	R^2
13.24	0.0278	0.9397	35.33	0.0056	0.9984

The kinetic plot of the adsorption of Pb (II) as a function of reaction time is shown in **Fig. 3.13** where triangle points are experimental data points and the solid line curve is the calculated curve.

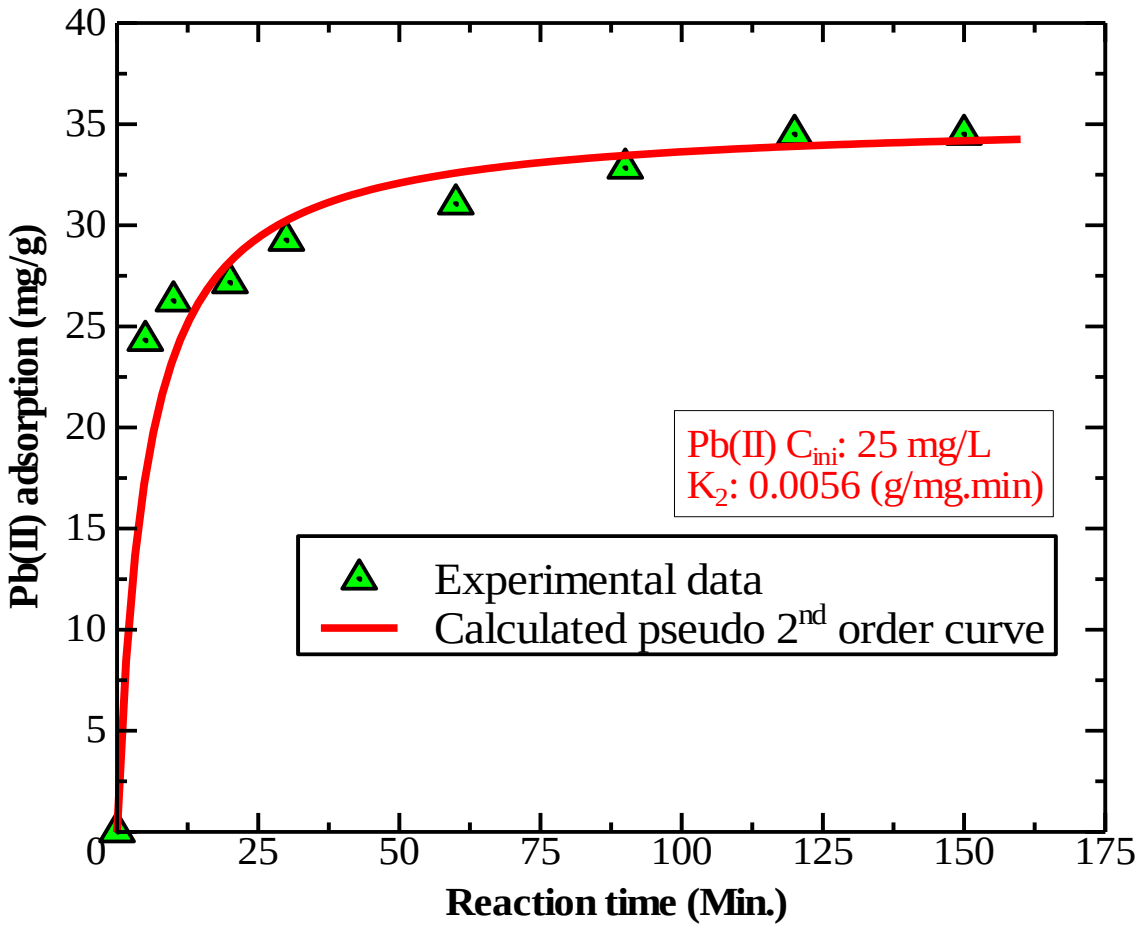

Fig. 3.13: The plot of adsorption of Pb (II) on zeolite as a function of time

It is very clear from the graph that the equilibrium reached in 120 minutes. It was found that the adsorption rate was rapid at first and then slowed down near the equilibrium state. After reaching the saturation point there was no significant change in the rate. The initial rapid increase in the rate was due to the availability of more number of active sites so that large number of Pb (II) got attached to adsorbent sites. As the time passed the number of active sites became less and finally the equilibrium state was obtained.

3.10 Test of Intraparticle Diffusion Model

To understand the mechanisms and rate controlling steps affecting the kinetics of adsorption, the kinetic experimental results were fitted to the Webber's intraparticle diffusion equation (mentioned in Introduction under the section **1.6**). The plot of Q_t verses $\sqrt{t}$ for the adsorption of Pb (II) on activated carbon zeolite is shown in **Fig. 3.14.** The

slope K_{id} (mg/g $min^{0.5}$) is the intraparticle diffusion rate constant, which can be evaluated from the slope of the linear plot of Q_t vs $t^{0.5}$ as shown in **Fig. 3.14**. The intercept of the plot reflects the boundary layer effect. The larger the intercept, the greater is the contribution of the surface adsorption in the rate controlling step. If the regression of Q_t vs $t^{0.5}$ is linear and passes through the origin, the intraparticle diffusion is the sole rate-limiting step. In present study, the linear plots (**Fig. 3.14)** at each concentration did not pass through the origin. This indicates that the intraparticle diffusion was not only rate controlling step which is in trend with the previous reports[54].

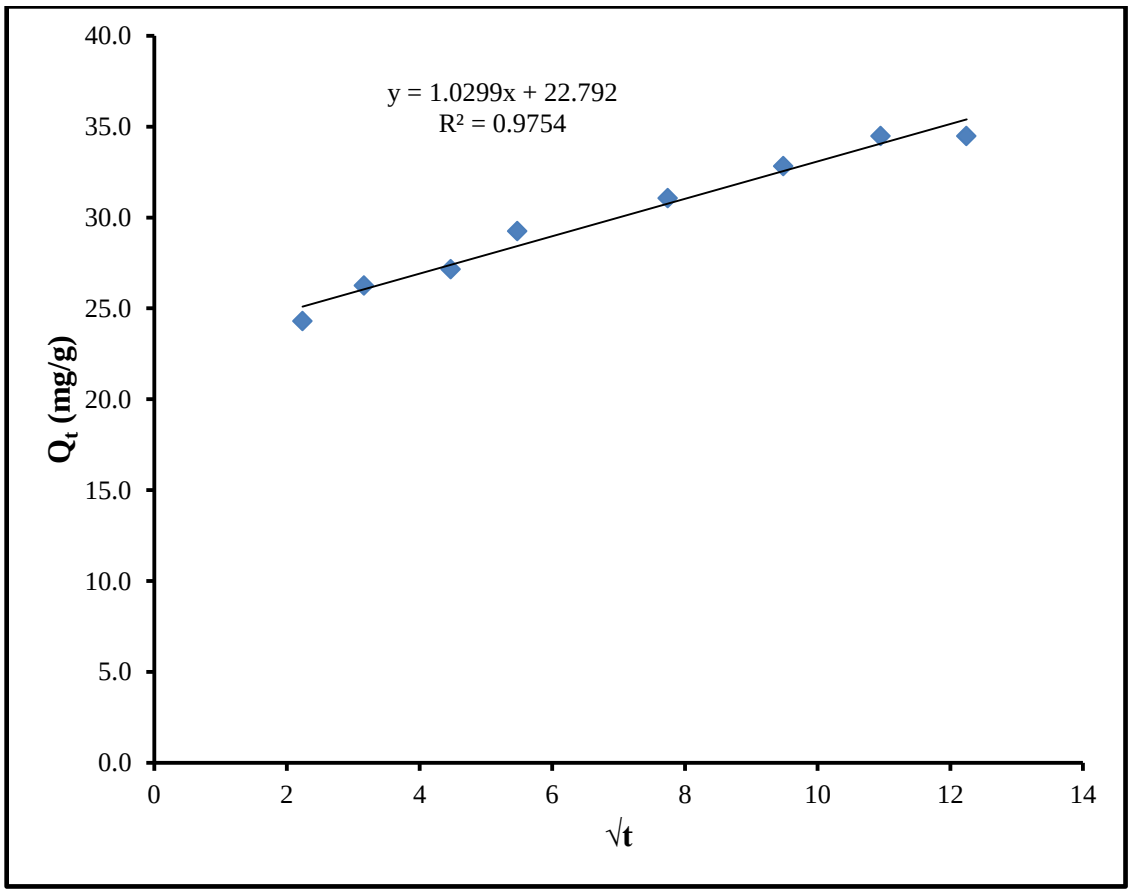

Fig. 3.14: Plot of Q_t verses √t for the adsorption of Pb (II) on activated carbon zeolite

3.11 Comparasion of Maximum Adsorption Capacity (Q_{max})

The comparison of maximum adsorption capacity (Q_{max}) of the activated carbon zeolite with earlier investigated adsorbent is tabulated below. The results reveal that activated

carbon zeolite possesses higher potentiality towards the adsorptive removal of Pb (II) from aqueous solution.

Table 3.5: **Comparison of maximum adsorption capacity (Q_{max}) of Pb (II) onto the activated carbon zeolite with earlier investigated adsorbent**

S.No.	**Adsorbent and Species**	**Q_{max} (mg/g)**	**Source**
1	Apricot stone material	21.38	[55]
2	γ -Alumina	65.67	[56]
3	European Black pine	27.53	[18]
4	Raw rice husk	131.81	[57]
5	Activated carbon prepared from sludge and sugarcane bagasse	51.30	[58]
6	Coal fly ash	5.52	[45]
7	Zeolite-P1	267.3	[46]
8	Linde type A Zeolite	37.59	[59]
9	Zeolite-X	549.3	[11]
10	Activated carbon-zeolite composite	270.27	[Present work]

.

CHAPTER 4

CONCLUSIONS

4.1 Conclusions

In the present work activated carbon-zeolite composite were prepared by activating coal fly ash (CFA) with NaOH at 650 ºC in N_2 atmosphere followed by heating at 80 ºC for 24 hrs. Thus prepared activated carbon zeolite composite were characterized by XRD analysis, FTIR and methylene blue adsorption method.

The XRD peaks at 2θ values of 33 and 35º were due to $NaAlO_2$ and 26-29 and 45º were due to $NaAlSiO_4$ which shows the strong evidence for the formation of zeolitic product. The AAS was employed for Pb analysis. The specific surface area of zeolitic product was found to be 241 m^2/g.

The optimum pH for the removal of lead with initial concentration of 25 ppm was found to be 6 with 94.00 % Pb (II) ion adsorption. The governing factors affect the adsorption characteristics of all adsorbents are competition of the H^+ ions with metal ions at low pH values which is shown by pH experiments. Adsorption isotherm study showed that the Langmuir model fitted better than Freundlich model. The maximum adsorption capacity of Pb (II) onto activated carbon-zeolite calculated from Langmuir model was 270.27 mg/g. The equilibrium contact time was found to be 120 minutes following the pseudo-second order kinetics model with rate constant value of 0.0056 g/(mg min).

The value of ΔG obtained from Langmuir equation was -24.00 kJ/mole. The negative value of free energy (ΔG) in adsorption process reveals the spontaneous nature and feasibility of the adsorption process for the adsorption of Pb (II) onto activated carbon-zeolite. The value of ΔG confirms the adsorption process is favored by physio-chemical adsorption. The value of χ^2 for the Langmuir model is smaller than that of the Freundlich model which concludes that adsorption of Lead (II) on activated carbon-zeolite follows the Langmuir adsorption isotherm. The value of the separation parameter K_L was found to be $0 \leq K_L \leq 1$ which revealed good adsorption of Lead (II) onto activated carbon-zeolite.

4.2 Suggestions for Further Work

Further investigations will be required to explain some aspects of zeolite synthesis that are still unclear in the current work, which could give better perspectives in terms of possible applications. Some recommendations for further studies are:

- The activated carbon zeolite can be used for the removal of hazardous metal ions from real waste water.
- By the use of autoclave several other desired zeolites can be prepared for targeted metal ion adsorption.
- The micro-mechanism of the adsorption of various hazardous ions on the adsorbents can be studied.
- Also a mathematical model of the mechanism of zeolite formation should be develop in order to provide a quantitative understanding on how zeolites nucleate and grow, which is fundamental from both a scientific and technological point of view.

References

1. Heidrich C., Feuerborn H. J., Weir A., Coal combustion products. A global perspective. *Journal of VGB PowerTech*, **2013**, 93, 46-52.
2. Jankowski J., Ward C. J., French D and Groves S., Mobility of trace element from selected Australian Fly ashes and its potential impacts on aquatic ecosystem. *Journal of Fuel*, **2006**, 85, 243-256.
3. Blissett R. S., Rowson N. A., A review of the multi-component utilization of coal fly ash. *Journal of Fuel*, **2012**, 97, 1-23.
4. Panitchakarn P., Laosiripojana N., Umpikul N and Pavasant P., Synthesis of high purity Na-A and Na-X zeolite from Coal fly ash. *Journal of the Air and Waste Management Association*, **2014**, 64, 586-596.
5. Chunfeng W., Jiansheng L., Xia S., Lianjun W., Xiuyun S., Evaluation of zeolites synthesized from fly ash as Potential adsorbents for wastewater containing heavy metals. *Journal of Environmental Sciences,* **2009**, 21(1), 127-136.
6. Weitkamp J., and Puppe L., Catalysis and zeolites: Fundamentals and Applications. Springer Science & Business Media, **2013**.
7. Wdowin M., Franus M., Panek R., Badura L., W Franus., The conversion technology of fly ash into zeolites. *Clean Technologies and Environmental Policy,* **2014**, 16(6), 1217-1223.
8. Auerbach S. M., Carrado K. A., Dutta P. K., Handbook of zeolite science and technology. CRC Press, **2003**.
9. Pavasant P., Klamrassamee T., Laosiripojana N., Synthesis of Zeolite from coal Fly ash: Its application as Water sorbent. *Journal of Engineering,* **2010**, 14, 44-37.
10. Jha V. K., Matsuda M., Miyake M., Sorption properties of the activated carbon-zeolite composite prepared from coal fly ash for Ni^{2+}, Cu^{2+}, Cd^{2+} and Pb^{2+}. *Journal of Hazardous Materials,* **2008,** 160, 148-153.
11. Jha V. K., Matsuda M and Michihiro M., Resource recovery from coal fly waste: an overview study. *Journal of the Ceramic Society of Japan*, **2008**, 116(2), 167-175.
12. Barrer R., Synthesis of zeolites. *Studies in Surface Science and Catalysis*, **1985**, **24**, 1-26.
13. Marcus B. K., and Cormier W. E., Going green with zeolites. *Journal of Chemical Engineering*, **1999**, **95**(6), 47-53.

14. Ribeiro F. R., Zeolites: science and technology, Springer Science and Business Media, **2012**.
15. Querol X., Moreno N., Umana J. C., Alastuey A., Hernandez E., LopezSoler A, Plana F., Synthesis of zeolites from Coal fly ash: an overview. *International Journal of Coal Geology*, **2002,** *50*, 413-423.
16. Xu R., Pang W., Yu J., Huo Q., Cheng J., Chemistry of zeolites and related porous materials: synthesis and structure. John Wiley & Sons, **2007**.
17. Acharya J., Sahu J. N., Mohanty C. R and Mikap B. C., Removal of lead (II) from wastewater by activated carbon developed from Tamarind wood activated with zinc chloride. *Journal of Chemical Engineering*, **2009**, 149, 249-262.
18. Momcilovic M., Purenovic M., Bojic A., Zarubica A and Randelovic M., Removal of lead (II) ions from aqueous solution by adsorption onto pine cone activated carbon. *Journal of Water Reuse and Desalination*, **2011**, 276, 53-59.
19. Ji L., Zhou L., Bai X., Shao Y., Zhao G., Yanzhi Q., Wang C and Li Y, Facial synthesis of multiwall carbon nanotubes iron oxides for removal of tetrabromobisphenol A and Pb (II). *Journal of Materials Chemistry*. **2012**, 22, 15853 -15862.
20. Sherchand O., Mehta K. D., Poudel P., Deo B and Baral N., Blood Lead levels of Primary school children in Kathmandu Municipility, Nepal. *Journal of Institute of Medicine*, **2014**, 36(3), 14-21.
21. Gedam A. H and Dongre R. S., Adsorption characterization of Pb (II) ion onto iodate doped chitosan composite: equilibrium and kinetics studies. *RSC Advances*, **2015**, 5, 54188-54201.
22. Ekka B., Rout L., Sahu M. K., Kumar A., Patel R. K and Das P., Removal efficiency of Pb (II) from aqueous solution by 1-alkyl-3-methylimidazolium bromide ionic liquid mediated mesoporous silica. *Journal of Environmental Chemical Engineering*, **2015**, 3(2), 1356-1364.
23. Li Y. H., Wang S., Wei J., Zhang S., Xu C., Luan Z., Wu D and Wei B., Lead adsorption on carbon Nanotubes. *Chemical Physics Letters*, **2002**, 357, 263-266.
24. Saleh T. A., Gupta V. K., and AL-Saadi A. A., Adsorption of lead ions from aqueous solution using porous carbon derived from rubber tire: Experimental and Computational Study. *Journal of Colloid and Interface Science*, **2013**, 396, 264-269.

25. Negi A. S., Anand S. C., A text Book of Physical Chemistry (1st edition), Wiley Eastern Limited, **1990**.
26. Ducan J. S., Introduction to Colloid and Surface chemistry, 3rd edition, Butterworth and Co. Ltd, **1980**.
27. Davis T. A., Volesky B., Vieira R. H. S. F., Sargassum Seaweed biosorbent for Heavy metal. *Water Research*, **2000**, 34(17), 4270-4278.
28. Jha V. K., Subedi K., Preparation of Activated Charcoal from Waste Tire. *Journal of Nepal Chemical Society*, **2011**, 27, 19-25.
29. Baral D. R., A dissertation submitted to Central Department of Chemistry, Tribhuvan University, **2011**, 18-20.
30. Langmuir I. J., The Adsorption of Gases on Plane Surfaces of Glass, Mica and Platinum. *Journal of American Chemical Society*, **1918**, 40(9), 1361-1403.
31. Maron S. H., Pruton C. F., Principles of Physical Chemistry (4thedition), Macmillan Company, New York, **2001**.
32. Freundlich H., Hetler W., *Journal of American Chemical Society*. **1939**, 61, 2228-2230.
33. Lagergreen S., Svenska B. R., *Veternskapsakad Handlinger*, **1898,** 24, 1-39.
34. Ho Y. S., Chiu W. T., Hsu C. S., Huang C. T., *Hydrometallurgy*, **2004,** 73, 55-61.
35. Weber W. J., Morris J. C., Kinetics of adsorption on carbon from solution. *Journal of Sanitary Engineering Division*, **1963**, 89(2), 31-60.
36. Aryal M., Ziagova M and Liakopoulou-Kyriakides M., Comparasion of Cr (VI) and As (V) removal is single and binary mixtures with Fe (III) treated Staphylococcus xylosus Biomass: Thermodynamic studies. *Journal of Chemical Engineering*, **2011**, 169, 100-106.
37. Agarwal A. K., Kadu M. S., Pandhurnekar C. P., Muthreja I. L., Langmuir, Freundlich and BET Adsorption Isotherm Studies for Zinc ions onto Coal Fly ash., *International Journal of Application or Innovation in Engineering and management*, **2014**, 3(1), 64-71.
38. Rajabzadeh M. A., Ghorbani Z., Keshavarzi B., Chemistry, mineralogy and distribution of selected trace-elements in the Parvadeh coals, Tabas, Iran. *Journal of Fuel*, **2016**, 174, 216-224.
39. Khadse S., Dawle Nisha., Patil P., Panhekar D., Zeolite synthesis from Coal fly ash: A Comprehensive Review of Literature. *International Research Journal of E nvironmental Science*, **2015**, 4(3), 93-99.

40. Basu. M., Pande M., Bhadoria P. B. S., and Mahapatra S. C., Potential fly-ash utilization in agriculture: A global review. *Journal of Progress in Natural Science*, **2009**, 19, 1173-1186.
41. Mukherjee A. B and Kikuchi R., Coal Ash from Thermal Power Plants in Finland. Biogeochemistry of Trace Elements in Coal and Coal Combustion Byproducts. *Journal of Recycling*, **2016**, 27, 59-76.
42. Khadse S., Panhekar D., Patil P., Synthesis of Zeolite using Fly ash and its application in Removal of Cu^{2+}, Ni^{2+}, Mn^{2+} from Paper Industry Effluent. *Research Journal of Chemical Sciences*, **2014**, 4(3), 5-9.
43. Guisnet M., Zeolites for Cleaner Technologies, Imperial College press, **2005**.
44. Yadla S. V., Sridevi. V., Chandana Lakshmi M. V. V., A Review on adsorption of Heavy metals from Aqueous Solution. *Journal of Chemical, Biological and Physical Sciences*, **2012**, 2(3), 1585-1593.
45. Muthreja I. L., Agarwal A. K., Kadu M. S and Pandhurnekar C. P., Adsorption and Kinetics behavior of fly ash used for the Removal of Lead (II) from an aqueous solution. *Journal of Chemical Technology and Metallurgy*, **2017**, 52(3), 505-512.
46. Lee M. N., Yi. G., Ahn B. J and Roddick F., Conversion of Coal Fly Ash into Zeolite and Heavy Metal Removal Characteristics of the Products. *Korean Journal of Chemical Engineering*, **2000**, 17(3), 325-331.
47. Ghimire K. N., Inoue K., Ohto K., Adsorptive Separation of Metallic pollutants onto Waste seaweeds, Porphyra Yezoensis and Ulva Japonica. *Journal of Separation Science and Technology*, **2007**, 42, 2003-2018.
48. Bernard B., Jimoh A., and Odigure J. O., Heavy metals removal from industrial Waste water by activated carbon prepared from Coconut shell. *Research Journal of Chemical Science*, **2013**, 3(8), 3-9.
49. Hawari A. H., Mulligan C. N., Biosorption of Lead (II), Cadmium (II), Copper (II) and Nickel (II) by Anaerobic Granular Biomass. *Journal of Bioresource Technology*, **2006**, 97, 692-700.
50. Shingh K. K., Talat M., Hasan S., Removal of Lead from Aqueous solutions by Agricultural Waste Maize Barn. *Journal of Bioresource Technol*ogy, **2006**, 97(16), 2124-2130.
51. EI-Wakil A. M., Abou EI-Matty W. M., Awad F. S., Removal of Lead from Aqueous solution on Activated carbon and Modified Activated carbon prepared

from Dry water Hyacinth Plant. *Journal of Analytical and BioAnalytical Techniques*, **2014**, 5, 187.

52. Basu M., Guha A. K and Ray L., Biosorptive removal of lead by lentil husk. *Journal of Environmental Chemical Engineering*, **2015,** 3, 1088-1095.
53. Huiping S., Huaigang C., Zepeng Zhang., Fangqui C., Adsorption properties of zeolites synthesized from coal fly ash for Cu (II). *Journal of Environmental Biology*, **2014**, 35, 983-988.
54. Hameed B. H., Salman J. M and Ahmad A. L., Adsorption Isotherm and Kinetic modeling of 2, 4-D pesticide on activated carbon derived from date stones. *Journal of Hazardous Materials,* **2009**, 163, 121-126.
55. Mouni L., Merabet D., Bouzaza A and Belkhiri L., Adsorption of Pb (II) from aqueous solutions using activated carbon developed from Apricot stone. *Journal of Desalination,* **2011**, 276, 148-153.
56. Bhat A., Megeri G. B., Thomas C., Bhargava H., Jeevitha C., Chandrasekhar S., and Madhu G. M., Adsorption and optimization studies of Lead from Aqueous solution using γ-Alumina. *Journal of Environmental Chemical Engineering,* **2015**, 3, 30-39.
57. Das V., Investigation on the Adsorption Behaviour of Lead (II) onto Rice Husk Powder. A dissertation submitted to Central Department of Chemistry, Tribhuvan University, **2012**.
58. Tao H. C., Zhang H.R., Li J. B., Ding W.Y., Biomass based Activated carbon obtained from sludge and sugarcane bagasse for removing Lead ion from waste water. *Journal of Bioresource Technology*, **2015**, 192, 611-617.
59. Payne K. B., Abdel-Fattah T. M., Adsorption of Divalent Lead Ions by zeolites and Activated carbon: Effects of pH, temperature and Ionic strength. *Journal of Environmental Science and Health*, **2004**, 39(9), 2275-229.

APPENDIX

Table A: Determination of λ_{max} of 5 mg/L methylene blue solution

S. No.	Wavelength (nm)	Absorbance
1	600	0.50
2	610	0.58
3	620	0.59
4	630	0.62
5	640	0.72
6	650	0.82
7	660	0.91
8	670	0.87
9	680	0.55
10	690	0.30

Table B: Calibration curve of the methylene blue solution

S.No.	Concentration (mg/L)	Absorbance
1	0	0.00
2	1	0.20
3	2	0.43
4	3	0.63
5	4	0.82
6	5	1.03
7	6	1.22
8	7	1.42
9	8	1.55
10	9	1.72
11	10	1.92

Table C: Adsorption of methylene blue solution on the surface of activated carbon zeolite [Total volume of methylene blue solution = 20 mL and Amount of adsorbent = 20 mg]

S.No.	Initial concentration C_i (mg/L)	Equilibrium concentration C_e (mg/L)	Amount Adsorbed Q_e (mg/g)	C_e/Q_e (g/L)
1	25	0.371	24.629	0.015
2	30	0.412	29.588	0.013
3	35	0.431	34.569	0.012
4	40	0.898	39.102	0.022
5	50	1.414	48.586	0.029
6	60	6.373	53.627	0.118
7	70	11.616	58.384	0.198
8	80	20.011	59.989	0.333
9	90	28.051	61.949	0.453
10	100	35.442	64.558	0.554

Table D: Calibration curve for Lead (II) ion solution

S.No.	Concentration (mg/L)	Absorbance
1	0	0.00
2	1	0.015
3	5	0.080
4	10	0.155

Table E: Effect of pH on Pb (II) ion adsorption onto activated carbon zeolite [Total volume of solution = 30 mL, Amount of adsorbent = 20 mg and Initial concentration = 25 mg/L, time = 24 hrs.]

S.No.	Initial pH	Initial concentration C_i (mg/L)	Equilibrium concentration C_e (mg/L)	Amount of Pb (II) adsorbed Q_e (mg/g)	Percentage adsorption (%)
1	2	25	8.51	24.73	65.96
2	3	25	6.61	27.58	73.56
3	4	25	4.41	30.88	82.36
4	5	25	2.98	33.03	88.08
5	6	25	1.50	35.25	94.00
6	7	25	5.42	29.37	78.32
7	8	25	7.11	26.83	71.56

Table F: Adsorption isotherm of Pb (II) ion onto activated carbon zeolite [Total volume of solution = 30 mL, Amount of adsorbent = 20 mg, optimum pH = 6 and time = 24 hrs.]

S.No.	Initial concentration C_i (mg/L)	Equilibrium concentration C_e (mg/L)	Amount of Pb (II) adsorbed Q_e (mg/g)	C_e/Q_e	Log C_e	Log Q_e
1	25	1.50	35.250	0.043	0.18	1.547
2	50	4.11	68.835	0.060	0.61	1.838
3	100	15.13	127.305	0.119	1.18	2.105
4	200	50.13	224.805	0.223	1.70	2.352
5	300	135.21	247.185	0.547	2.13	2.393
6	400	230.98	253.530	0.911	2.36	2.404
7	500	325.55	261.675	1.244	2.51	2.418
8	600	423.21	265.185	1.596	2.63	2.424

Table G: Kinetics studies of Pb (II) ion adsorption onto activated carbon zeolite [Total volume of solution = 30 mL, Initial concentration = 25 mg/L, Amount of adsorbent = 20 mg and optimum pH = 6]

Time (min)	Square root of time (√t)	Initial Concen. C_i (mg/L)	Equilibrium Concen. C_e (mg/L)	Amount of Pb (II) ion adsorbed Q_t (mg/g)	t/Q_t, (min/ mg/g	Q_e-Q_t	Log(Q_e- Q_t)
5	2.236	25	8.80	24.3	0.205	10.41	1.017
10	3.162	25	7.50	26.25	0.380	8.46	0.927
20	4.472	25	6.90	27.15	0.736	7.56	0.878
30	5.477	25	5.50	29.25	1.025	5.46	0.737
60	7.745	25	4.30	31.05	1.932	3.66	0.563
90	9.486	25	3.12	32.82	2.742	1.89	0.276
120	10.954	25	2.01	34.48	3.480	0.23	-0.638
150	12.247	25	2.01	34.48	4.350	0.23	-0.638
24hrs	-	25	1.50	35.25	-	0.00	-

Table H : Chi square test for Langmuir parameter

S.No.	Initial concentration C_i (mg/L)	Equilibrium concentration C_e (mg/L)	Q_e (mg/g) Experimental	Q_e (mg/g) calculated From Langmuir model	$\frac{(Q_{e,calc} - Q_{e,exp})^2}{Q_{e,calc}}$
1	25	1.50	35.250	28.011	1.870
2	50	4.11	68.835	65.031	2.225
3	100	15.13	127.305	145.508	2.277
4	200	50.13	224.805	214.707	0.474
5	300	135.21	247.185	246.609	0.001
6	400	230.98	253.530	255.897	0.021
7	500	325.55	261.675	259.912	0.145
8	600	423.21	265.185	262.231	0.033
$x^2 = \sum \frac{(Q_{e,calc} - Q_{e,exp})^2}{Q_{e,calc}}$					0.880

Table I: Chi square test for Freundlich parameter

S.No.	Initial concentration C_i (mg/L)	Equilibrium concentration C_e (mg/L)	Q_e (mg/g) Experimental	Q_e (mg/g) calculated From Freundlich model	$\frac{(Q_{e,calc} - Q_{e,exp})^2}{Q_{e,calc}}$
1	25	1.50	35.250	47.072	2.970
2	50	4.11	68.835	66.636	0.0726
3	100	15.13	127.305	104.440	5.006
4	200	50.13	224.805	157.863	28.387
5	300	135.21	247.185	222.330	2.779
6	400	230.98	253.530	267.917	0.772
7	500	325.55	261.675	300.401	4.992
8	600	423.21	265.185	328.851	12.326
$x^2 = \sum \frac{(Q_{e,calc} - Q_{e,exp})^2}{Q_{e,calc}}$					7.163